



Calhoun: The NPS Institutional Archive
DSpace Repository

Theses and Dissertations

1. Thesis and Dissertation Collection, all items

1976

Laser doppler anemometer measurement and analytical comparison of flow around a cylinder at low Reynolds number.

Wanner, Terry Scott

Monterey, California. Naval Postgraduate School

<http://hdl.handle.net/10945/17832>

Downloaded from NPS Archive: Calhoun



<http://www.nps.edu/library>

Calhoun is the Naval Postgraduate School's public access digital repository for research materials and institutional publications created by the NPS community. Calhoun is named for Professor of Mathematics Guy K. Calhoun, NPS's first appointed -- and published -- scholarly author.

Dudley Knox Library / Naval Postgraduate School
411 Dyer Road / 1 University Circle
Monterey, California USA 93943

LASER DOPPLER ANEMOMETER MEASUREMENT AND
ANALYTICAL COMPARISON OF FLOW AROUND A
CYLINDER AT LOW REYNOLDS NUMBER

Terry Scott Wanner

DUNLEY KNOX LIBRARY
NAVAL POSTGRADUATE SCHOOL
MONTEREY, CALIFORNIA 93940

NAVAL POSTGRADUATE SCHOOL

Monterey, California



THESIS

Laser Doppler Anemometer Measurement and
Analytical Comparison of Flow Around a
Cylinder at Low Reynolds Number

by
Terry Scott Wanner

March 1976

Thesis Advisor:

D. J. Collins

Approved for public release; distribution unlimited.

T175040

SECURITY CLASSIFICATION OF THIS PAGE (When Data Entered)

REPORT DOCUMENTATION PAGE

READ INSTRUCTIONS
BEFORE COMPLETING FORM

1. REPORT NUMBER		2. GOVT ACCESSION NO.	3. RECIPIENT'S CATALOG NUMBER
4. TITLE (and Subtitle) Laser Doppler Anemometer Measurement and Analytical Comparison of Flow Around a Cylinder at Low Reynolds Number		5. TYPE OF REPORT & PERIOD COVERED Master's Thesis March 1976	
7. AUTHOR(s) Terry Scott Wanner		6. PERFORMING ORG. REPORT NUMBER	
9. PERFORMING ORGANIZATION NAME AND ADDRESS Naval Postgraduate School Monterey, California 93940		8. CONTRACT OR GRANT NUMBER(s)	
11. CONTROLLING OFFICE NAME AND ADDRESS Naval Postgraduate School Monterey, California 93940		10. PROGRAM ELEMENT, PROJECT, TASK AREA & WORK UNIT NUMBERS	
12. REPORT DATE March 1976		13. NUMBER OF PAGES 61	
14. MONITORING AGENCY NAME & ADDRESS (if different from Controlling Office) Naval Postgraduate School Monterey, California 93940		15. SECURITY CLASS. (of this report) Unclassified	
16. DISTRIBUTION STATEMENT (of this Report) Approved for public release; distribution unlimited.		15a. DECLASSIFICATION/DOWNGRADING SCHEDULE	
17. DISTRIBUTION STATEMENT (of the abstract entered in Block 20, if different from Report)			
18. SUPPLEMENTARY NOTES			
19. KEY WORDS (Continue on reverse side if necessary and identify by block number) LDV Laser Doppler Velocimeter			
20. ABSTRACT (Continue on reverse side if necessary and identify by block number) In this study, the flow characteristics of air around a circular cylinder were determined by two means: by analytical solution of the Navier-Stokes equations, and actual measurement of the flow itself. A DISA LD 5586 laser doppler anemometer system was employed to measure normal (v) and parallel (u) velocity components of a laminar flow regime about a three-sixteenths inch diameter cylinder mounted in a 32 x 45 inch wind tunnel (Reynolds number approximately 40).			

A finite element grid was constructed using triangular elements which encompassed the upper half-cylinder. Flow measurements using the laser velocimeter were confined to this region of interest.

Theory was compared against experimental results, and the feasibility of the utilization of this particular type of laser anemometer was evaluated.

Laser Doppler Anemometer Measurement and Analytical
Comparison of Flow Around a Cylinder
at Low Reynolds Number

by

Terry Scott Wanner
Lieutenant, United States Navy
B.S., United States Naval Academy, 1969

Submitted in partial fulfillment of the
requirements for the degree of

MASTER OF SCIENCE IN AERONAUTICAL ENGINEERING

from the

NAVAL POSTGRADUATE SCHOOL
March 1976

I. ABSTRACT

In this study, the flow characteristics of air around a circular cylinder were determined by two means: by analytical solution of the Navier-Stokes equations, and actual measurement of the flow itself. A DISA LD 5586 laser doppler anemometer system was employed to measure normal (v) and parallel (u) velocity components of a laminar flow regime about a three-sixteenths inch diameter cylinder mounted in a 32 x 45 inch wind tunnel (Reynolds number approximately 40).

A finite element grid was constructed using triangular elements which encompassed the upper half-cylinder. Flow measurements using the laser velocimeter were confined to this region of interest.

Theory was compared against experimental results, and the feasibility of the utilization of this particular type of laser anemometer was evaluated.

TABLE OF CONTENTS

I.	ABSTRACT	3
II.	DESCRIPTION OF LASER ANEMOMETER	6
III.	ANALYTICAL DERIVATION	14
IV.	DESCRIPTION OF EXPERIMENT	22
V.	DESCRIPTION OF COMPUTER PROGRAM	28
VI.	ANALYSIS OF RESULTS	31
	A. ERROR ANALYSIS	34
VII.	CONCLUSION	35
	APPENDIX A LDV data	36
	COMPUTER PROGRAM	38
	BIBLIOGRAPHY	61

II. DESCRIPTION OF LASER ANEMOMETER

A basic laser anemometer is comprised of four primary elements:

- (1) a coherent light source
- (2) optics
- (3) signal converter (photomultiplier tube)
- (4) signal processor/display

The principle of the laser anemometer is to create a grid pattern and measure the speed with which a particle in a fluid free stream passes through the grid. The following assumptions were taken into consideration:

- (1) particles injected into the free stream are small enough to faithfully follow stream lines of the flow, thus by measuring particle characteristics, we are actually measuring the medium's characteristics. This is easily achieved by use of particles which are on the order of a few microns in diameter.
- (2) particle generation results in a consistent particle size, or at least a majority of the particles are within a specified range of sizes. For example, DOP (di-2-ethylhexyl phthalate) particle generators produce particles with a mean diameter of 0.75 microns and burning turbine oil produces particles on the order of 4-6 microns (from electron microscope).

A laser is incorporated because of its coherency and power. The aforementioned grid is in reality the result of two coherent beams interfering with themselves (Fig. 1). The optics produce the beam pair by conventional splitting and focusing. Because the laser beam intensity is of a Gaussian distribution the grid created by constructive and destructive interference is not uniform over the entire focal volume. The fringes created on the outer portions of the horizontal axis are not perfectly formed because of slightly different intensities in that area. The main portion of the interference grid is uniform and, most importantly, the fringe spacing (D_f) is determined only by the laser wavelength (λ) and the half angle of the beam pair convergence ($\theta/2$).

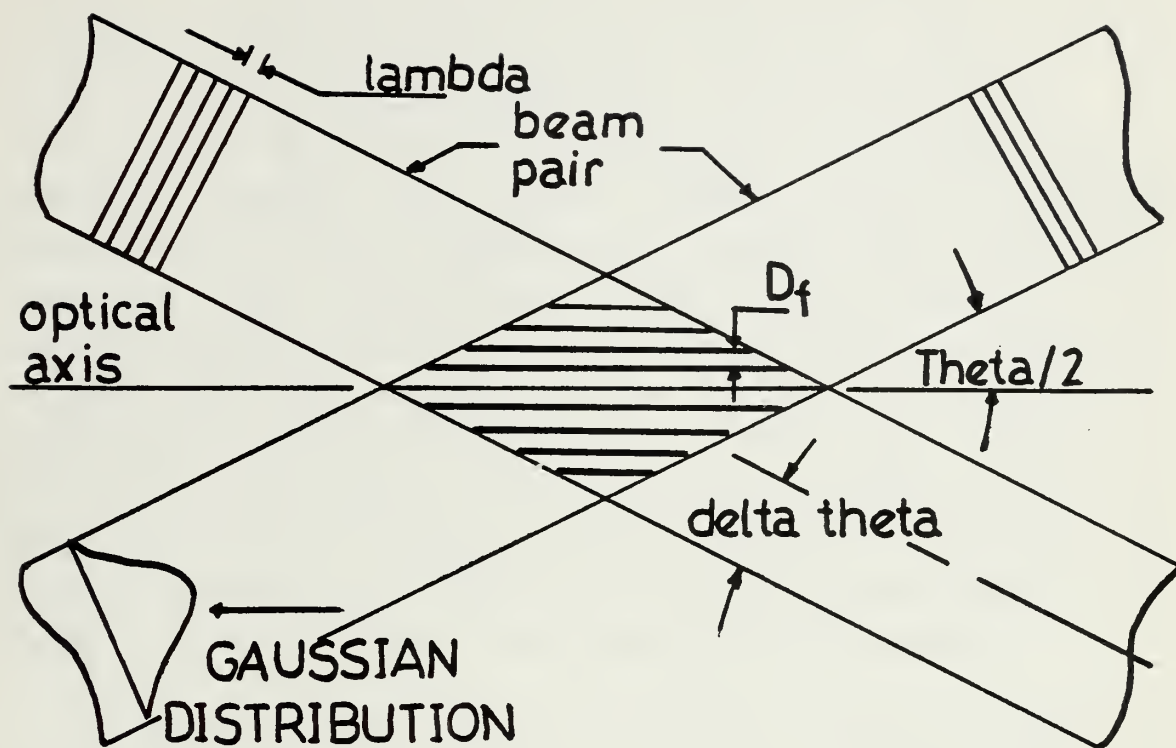
$$D_f = \lambda / (2 \sin(\theta/2))$$

The number of fringes (N_f) may also be computed, provided the beam focusing convergence angle ($\Delta \theta$) is known, by the relation:

$$N_f = 8 \tan(\theta/2) / (\pi \Delta \theta)$$

The number of fringes is important only to ensure that the signal processing apparatus will receive enough information to make possible further data reduction. If an insufficient number of fringes exists, not enough signal will be available for velocity determination.

Solid particles with a mean diameter which is less than half the fringe spacing are introduced into the free stream



FRINGE PATTERN GEOMETRY

Figure 1

of the fluid to be measured. When the particle is small compared to the fringe spacing the scattered light exhibits essentially 100% modulation, while particles equal to the fringe spacing produce negligible modulation[Ref. 2]. The particles may be produced by atomization of water, dop-air reaction, burning oil, smoke bombs, or may be bought commercially, as e.g. polystyrene spheres and some solid chemicals such as zinc oxide. Choice of the particle to be used is normally dictated by the fringe spacing in the focal volume, and the nature of the medium to be measured. Regardless of choice, the particle must be small enough to follow the streamlines as closely as possible, because the laser anemometer actually measures the particle velocity and unless the particle's motion is a true representation of the fluid velocity, pertinent data may not be obtained.

Inside the measuring (or focal) volume, bands of darkness and brightness exist due to the interference of the two beams. Particles entering the focal volume will alternately scatter light as they pass through regions of constructive interference (typical focal volume dimensions are 300 microns wide by 4 millimeters long and contain approximately 64 fringes). A photomultiplier tube located on the optical axis and focused into the measuring volume receives this scattered light and converts what appears to be a modulated light signal into a series of voltage pulses. Each voltage pulse correlates to a particle crossing one fringe. Because the spacing of the fringes is known, the frequency of the voltage pulse train may be equated to the velocity of the particle by the following relationship:

$$f = V_0 / D_f = 2 * V_0 * \sin(\Theta/2) / \lambda$$

where D_f is the fringe spacing and V_0 is the velocity of the

particle. Now the processor is left with a fairly simple task of counting the frequency and multiplying it by a calibration factor, which is, in essence, a fringe spacing parameter to arrive at a velocity.

As long as we are assured that only one particle is in the measuring volume at one time, the apparatus will operate correctly, but this is an unrealistic assumption. In order to achieve such a situation, the seeding density of the particles would be exceptionally sparse and the resulting data rate would be so slow as to preclude timely data reduction. To overcome this obstacle, a validation circuit is incorporated into the counter/processor. When a particle crosses a fringe spacing, two counters are triggered. One measures the time duration for five fringe crossings and holds this information. The second counter continues to measure the time for a total of eight fringe crossings. The time of the first counter is then compared with that of the second counter, and if the first time is indeed five-eighths of the second time (within specified limits, i.e., comp. accuracy) a validation gate is opened and the resultant frequency is then stored into an ensemble cell. The ensemble cell is adjustable to hold various numbers of counts and average them for the final velocity display. The final displayed velocity then is that component of fluid velocity which is perpendicular to the optical axis and contained in the same plane as the beam pair (Fig. 2).

The anemometer may be operated in three modes: reference beam, forward scatter, and back scatter. The last two modes are most frequently employed and are described here:

Forward scatter mode: in this mode, the photomultiplier tube is located on the optical axis and focused in a direction directly opposed to the direction of the emerging beam pairs. This mode offers the strongest attainable

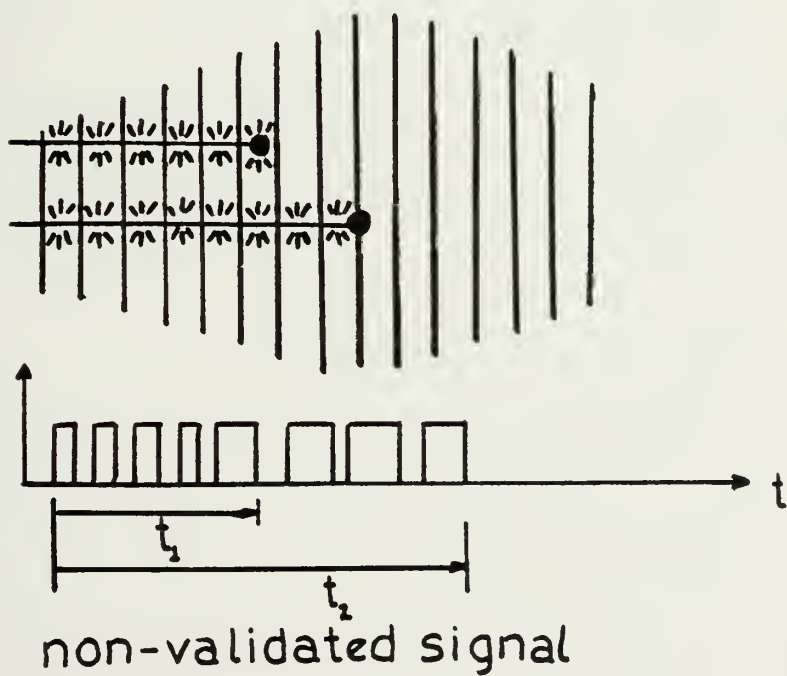
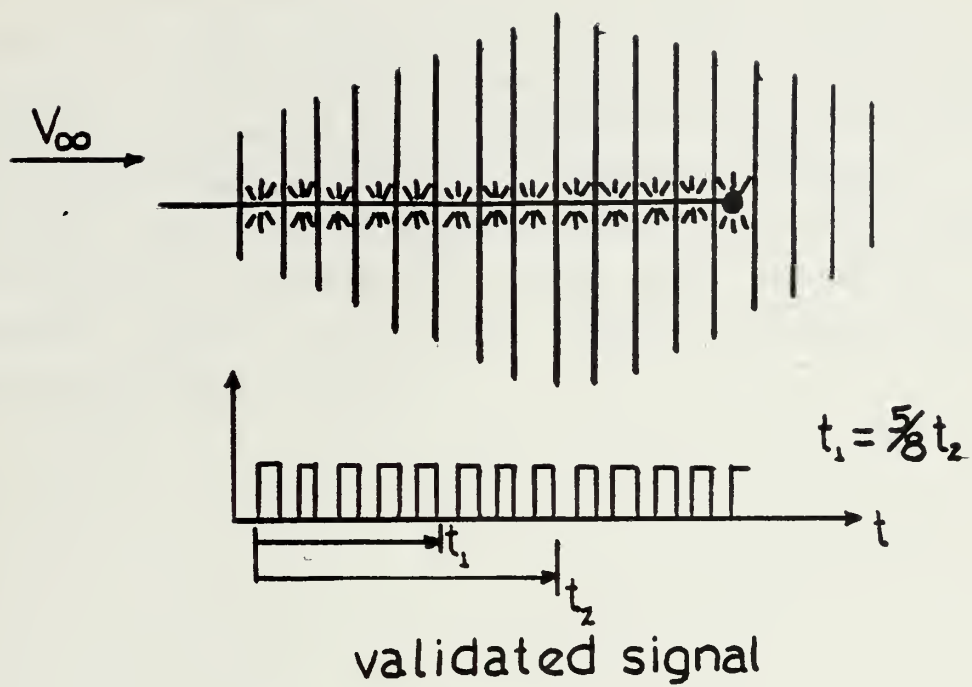
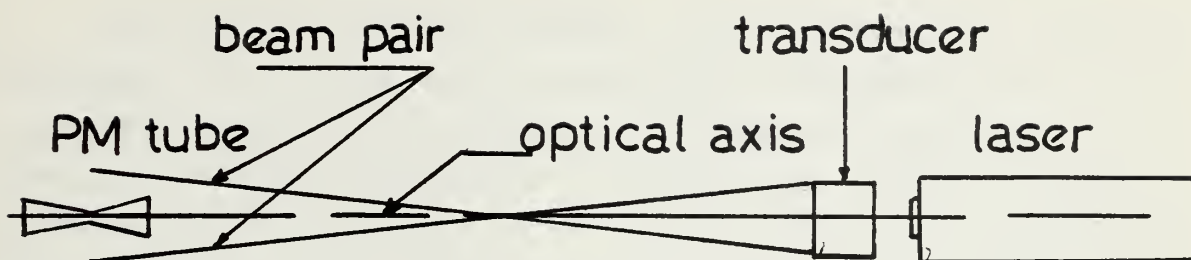


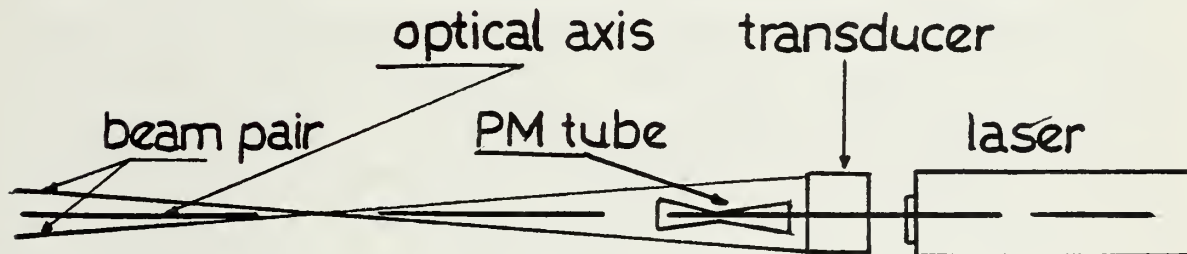
Figure 2

signal.

Back scatter mode: again the photomultiplier tube is mounted on the optical axis, but now it is aligned in the direction of the emerging beam pairs. This mode affords the ability to measure fluid velocities in confined spaces or in situations where the detector cannot be mounted in forward scatter, such as in measuring velocities in a compressor. Additionally, operation in this mode requires a higher powered laser due to the reduced intensity of back scattered light (Fig. 3).



LDV FORWARD SCATTER MODE



LDV BACK SCATTER MODE

Figure 3

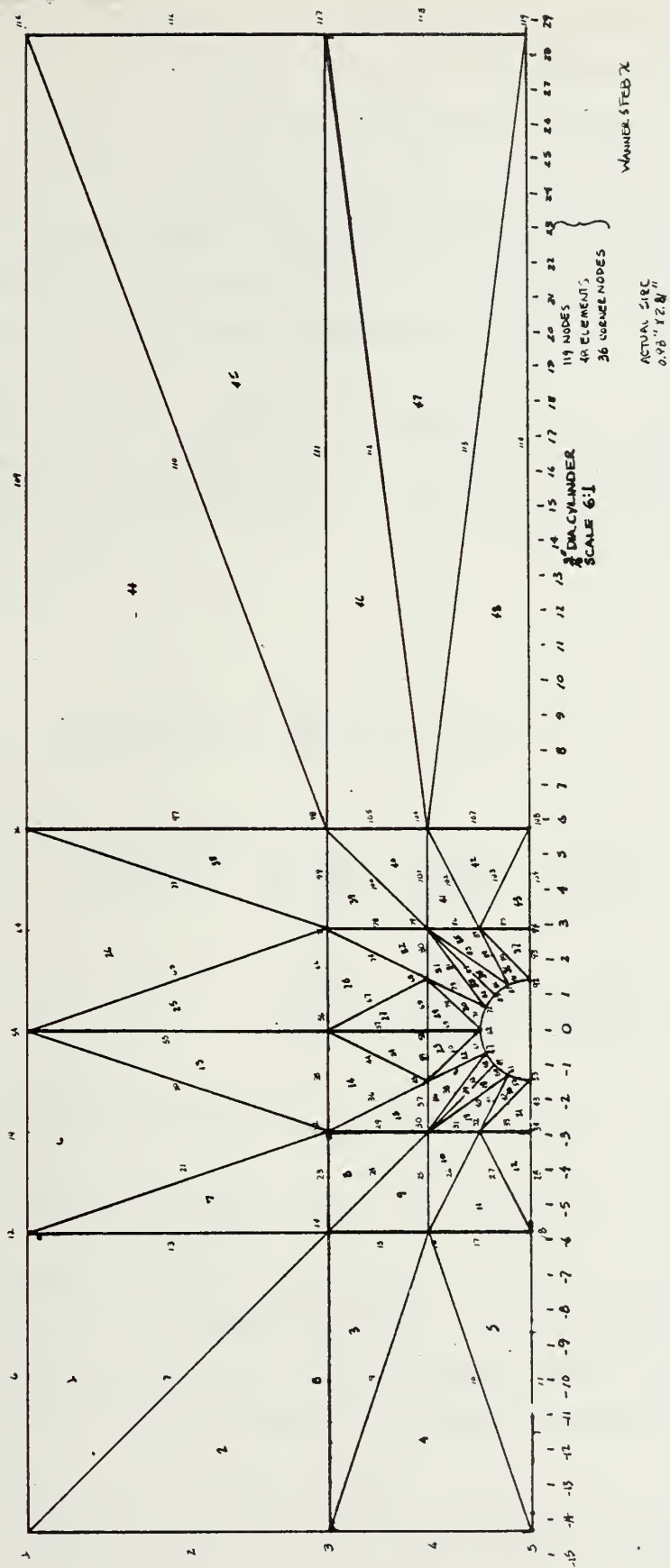
III ANALYTICAL DERIVATION

The finite element method is a numerical analysis technique for obtaining approximate solutions to a wide variety of engineering problems. It offers a means to solve complex continuum problems by sub-dividing them into simpler interrelated problems. The nature of this engineering problem does not readily lend itself to a closed form solution. Therefore a numerical solution is dictated.

The method of finite elements is well employed where there are irregular geometries or unusual specifications of boundary conditions. The method gives a piecewise approximation to the governing equations. Figure 4 shows the finite element grid employed in this flow problem. Approximating functions (interpolation functions) are defined in terms of the values of the field variables at the nodes. For the finite element representation, the nodal values of the field variables become the new unknowns and, once found, the interpolation functions define the field variable throughout the field of elements. The degree of the interpolation polynomials is governed by the number of nodes per element and dictated by the order of the governing equations.

The basic principle of the finite element method is to divide the solution domain into a finite number of subdomains (elements) which are connected only at node points. Interpolation polynomials are created for each element and a collection of interpolation functions over the whole solution domain provide a piecewise approximation to the field variable.

Introduction of generalizations facilitate direct derivation of finite element equations from governing differential equations. The method of weighted residuals



Finite element grid

Figure 4

(Galerkin's Method) is a technique for obtaining approximate solutions to non-linear partial differential equations. We first assume the general function behavior of the dependent field variable in some way so as to approximately satisfy the given differential equations and boundary conditions. After applying this approximation to the original equations, some error will result, which we desire to minimize or drive to zero over the entire solution domain.

The basic set of differential equations governing the problem from a velocity and pressure formulation approach are (after linearization by approximating non-linear viscous terms u_n, v_n):

$$\text{continuity} \quad \frac{\partial u}{\partial x} + \frac{\partial v}{\partial y} = 0$$

$$\text{momentum} \quad u_n \frac{\partial u}{\partial x} + v_n \frac{\partial u}{\partial y} = -\frac{1}{\rho} \frac{\partial P}{\partial x} + \nu \nabla^2 u$$

$$u_n \frac{\partial v}{\partial x} + v_n \frac{\partial v}{\partial y} = -\frac{1}{\rho} \frac{\partial P}{\partial y} + \nu \nabla^2 v$$

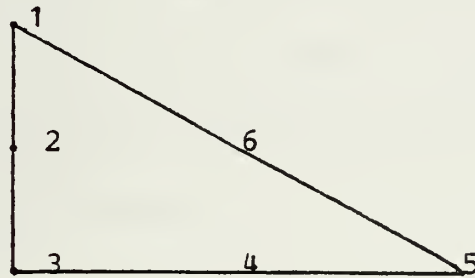
u_n, v_n , and P_n are approximate solutions to the flow problem

and may be visualized as the n^{th} iteration of the procedure of solution. These equations used in formulation of the problem are by no means unique. Stream functions and stream function with vorticity formulations have also been employed to establish finite element solution procedures.

Inasmuch as the velocity terms are of second order, a second order interpolation polynomial must be used to

calculate these unknowns. The pressure terms are of first order and hence require only first order interpolation.

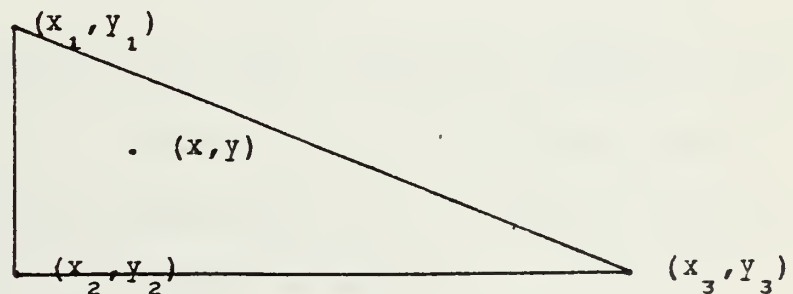
The basic element chosen for this solution was the triangle and, in a localized scheme, is visualized as follows:



Nodes 2, 4 and 6 lie equidistant between their respective corner nodes.

Nodes 1, 3, and 5 are referred to as corner nodes and are the basis for the linear interpolation polynomials derived for the pressure terms. For any triangular element, the corner nodes are described by their Cartesian coordinates x_i, y_i .

Consider the following local element:



The coordinates of node one are x_1, y_1 ; node two x_2, y_2 ; etc. and the interior point (x, y) may be described as a linear combination of the three corner nodes:

$$x = L_1 x_1 + L_2 x_2 + L_3 x_3$$

$$y = L_1 y_1 + L_2 y_2 + L_3 y_3$$

where L_i is the natural coordinate (interpolation polynomial, here linear) or weighting function which relates the coordinates of the corner nodes to any interior node. L_i has a value of one at the point x_i, y_i and is zero at the other two nodes of the element.

The L_i 's expressed as linear functions of the Cartesian coordinates then are

$$L_1(x, y) = \frac{1}{2\Delta} (a_1 + b_1 x + c_1 y)$$

$$L_2(x, y) = \frac{1}{2\Delta} (a_2 + b_2 x + c_2 y)$$

$$L_3(x, y) = \frac{1}{2\Delta} (a_3 + b_3 x + c_3 y)$$

$$\text{where } 2\Delta = \begin{vmatrix} 1 & x_1 & y_1 \\ 1 & x_2 & y_2 \\ 1 & x_3 & y_3 \end{vmatrix}$$

which is equal to the area of the triangular element and $a_1 = x_2 y_3 - x_3 y_2$, $b_1 = y_2 - y_3$, and $c_1 = y_1 - y_2$, the determinants of the minors corresponding coefficients a_1 , b_1 , or c_1 , and the other coefficients are similarly computed.

For the velocity terms, second order interpolation polynomials are indicated, while the pressure terms remain first order. Hence the introduction of more nodes (6) will result in a new set of weighting functions which may also be

expressed in terms of the natural coordinate interpolation polynomials:

$$N_1 = 2L_1^2 - L_1$$

$$N_2 = 4L_1 L_2$$

$$N_3 = 2L_2^2 - L_2$$

$$N_4 = 4L_2 L_3$$

$$N_5 = 2L_3^2 - L_3$$

$$N_6 = 4L_1 L_3$$

$$N_i^P = L_i$$

$$u^e = \sum_i^6 N_i u_i$$

$$v^e = \sum_i^6 N_i v_i$$

$$P^e = \sum_i^3 N_i^P P_i \quad (xxxx)$$

Application of Galerkin's Method to the governing equations results in the following integral expressions:

$$-\int_{\Omega} N_i \left(u_n \frac{\partial u}{\partial x} + v_n \frac{\partial u}{\partial y} + \frac{1}{\rho} \frac{\partial P}{\partial x} - \nu \nabla^2 u \right) d\Omega = 0$$

$$-\int_{\Omega} N_i \left(u_n \frac{\partial v}{\partial x} + v_n \frac{\partial v}{\partial y} + \frac{1}{\rho} \frac{\partial P}{\partial y} - \nu \nabla^2 v \right) d\Omega = 0$$

$$\int_{\Omega} N_i^{(P)} \left(\frac{\partial u}{\partial x} + \frac{\partial v}{\partial y} \right) d\Omega = 0$$

here Ω implies "over the area of the triangle".

Then we may make the substitution of the field variable in terms of x and y into terms of L_i .

$$\text{e.g.:} \quad \text{given} \quad u(x,y) \Leftrightarrow u(L_i)$$

$$\text{then} \quad \frac{\partial u}{\partial x} = u^e \frac{\partial N_i}{\partial L_i} \frac{\partial L_i}{\partial x}$$

$$\text{where} \quad \frac{\partial L_i}{\partial x} = \frac{b_i}{2\Delta}$$

$$\text{and a similar procedure for} \quad \frac{\partial u}{\partial y} = u^e \frac{\partial N_i}{\partial L_i} \frac{\partial L_i}{\partial y}$$

where $\frac{\partial \bar{c}_i}{\partial y} = \frac{c_i}{2\Delta}$

Substitution of equations (xxxx) into u^e , v^e and P^e and application of the above chain rule allows integration by parts:

$$K_1 = \int \left[\frac{\mu}{\rho} \left(\frac{\partial N_i}{\partial x} \frac{\partial N_j}{\partial x} + \frac{\partial N_i}{\partial y} \frac{\partial N_j}{\partial y} \right) - u^{(e)} N_i \frac{\partial N_j}{\partial x} - v^{(e)} N_i \frac{\partial N_j}{\partial y} \right] dx dy$$

$$K_2 = - \int N_j^{(r)} \frac{\partial N_i}{\partial x} dx dy$$

$$K_3 = - \int N_j^{(m)} \frac{\partial N_i}{\partial y} dx dy$$

The evaluated integral expressions then form the influence matrix as follows:

$$\begin{bmatrix} K_1 & 0 & K_2 \\ 0 & K_1 & K_3 \\ K_2 & K_3 & 0 \end{bmatrix}$$

Specification of the field variables or right hand sides of the matrix equation then provides a defined problem:

$$[TM] \cdot [T] = [Q]$$

Additionally, evaluation of the integral expressions yields boundary terms which must be computed for nodes which lie on the boundary of the control surface:

$$R_1 = \int N_i X^* ds \quad R_2 = \int N_i Y^* ds$$

$$\text{where } X^* = \mu \nabla u^{(e)} \cdot \hat{n} - \hat{n}_x P^{(e)} \quad \text{and} \quad Y^* = \mu \nabla v^{(e)} \cdot \hat{n} - \hat{n}_y P^{(e)}$$

It should be noted that along vertical boundaries there is

no outward pointing normal \hat{n}_y and similarly along horizontal boundaries no \hat{n}_x exists, and furthermore these terms are not computed where u and v are specified. Additionally, it was assumed that along the left-and right-hand side and upper boundaries $\partial u / \partial x$ and $\partial v / \partial y$ were identically equal to zero because these boundaries were placed at five or more characteristic lengths (diameters) from the cylinder and considered to be outside the realm of influence of the flow about the cylinder.

The terms comprising K_1 , K_2 and K_3 are entered element by element into the main program in steps FLU02080 through QZ00170. Then each element's matrix is compiled into the field matrix (comprised of all elemental matrices) and is solved iteratively to output the horizontal velocity component u , the vertical component v , and the pressure P at every node in the field.

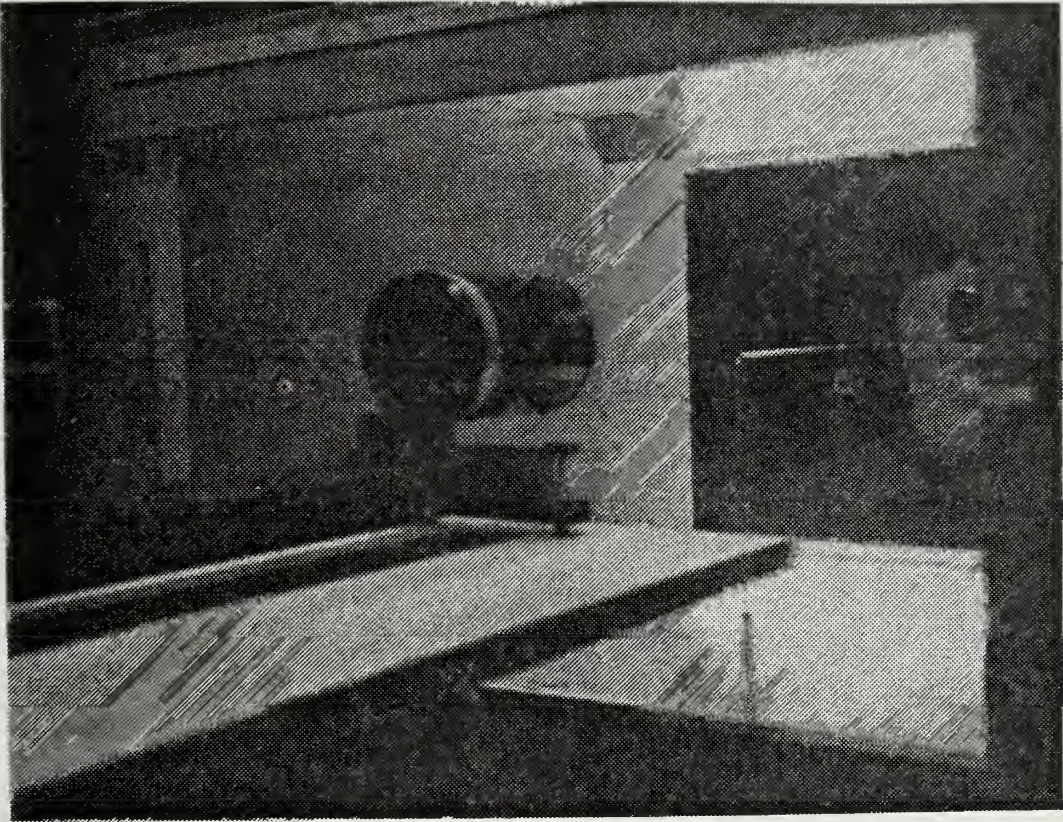
IV. DESCRIPTION OF EXPERIMENT

A right-angled, three-sixteenths inch cylinder made of stainless steel was mounted in an AEROLAB series 90 32x45 inch low speed wind tunnel through the floor of the test section (Fig. 5). The portion of the rod protruding down through the test section was mounted on a two-degree-of-freedom, micrometer controlled bed which allowed the rod to be maneuvered in the vertical plane parallel to the flow direction. This scheme enabled the laser velocimeter and photomultiplier tube to be mounted, aligned and left undisturbed for the entire period during which data were taken. The bed was positioned to read locations in the control volume which directly coincided with the location of the nodes in the finite element mesh (Fig. 6).

In the interest of precluding as many opportunities for error as possible, all u velocity components were first read and then components in a forty-five degree position were taken thus necessitating only one re-orientation of the beam pairs.

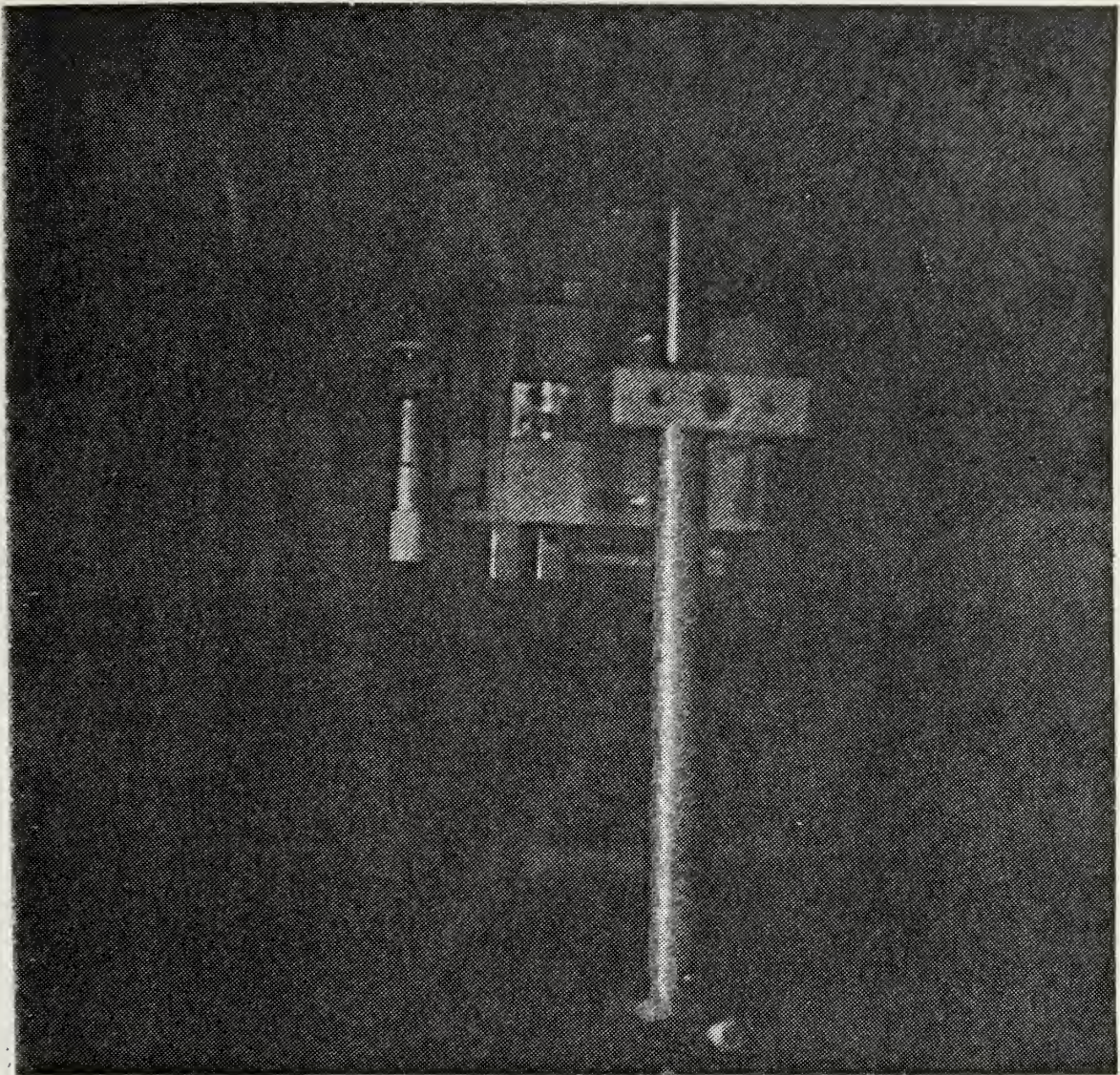
The plexiglass window prefacing the optics transducer of the test section had one-quarter inch holes drilled into it to allow the beam pairs to pass unimpeded, thereby minimizing distortion of the focal volume fringe pattern. The photomultiplier tube was likewise accommodated through the far window.

The seeding mechanism employed zinc-hexachloroethane based (non-toxic) white smoke bombs. The nature of the closed return wind tunnel permitted continuous measurement without interruption for re-seeding of the flow. By means of electron microscopy, the average size of the smoke particles was determined to be on the order of two microns (Fig. 7).



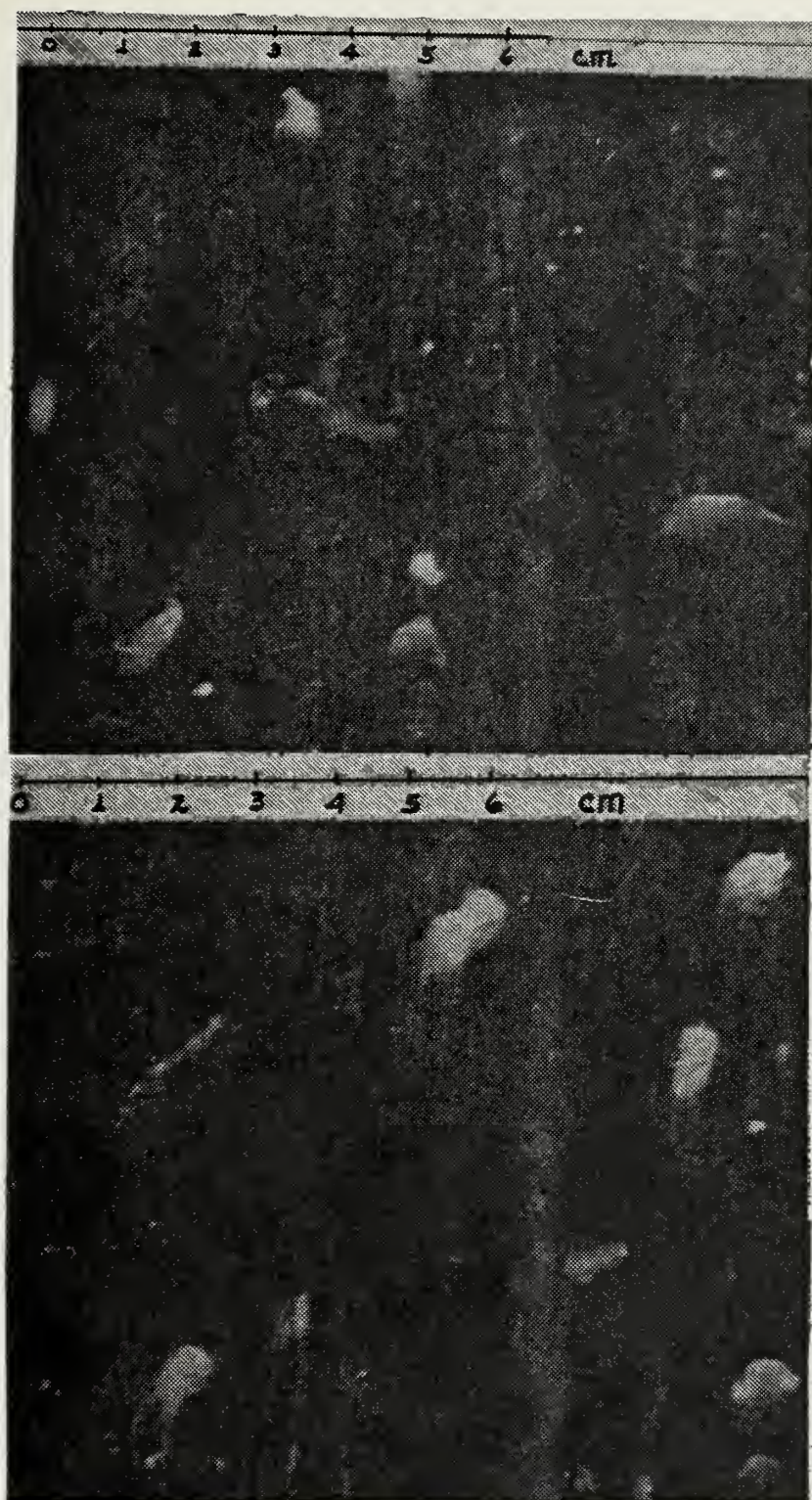
Cylinder mounted in wind tunnel and LDV setup.

Figure 5



Traversing mechanism

Figure 6

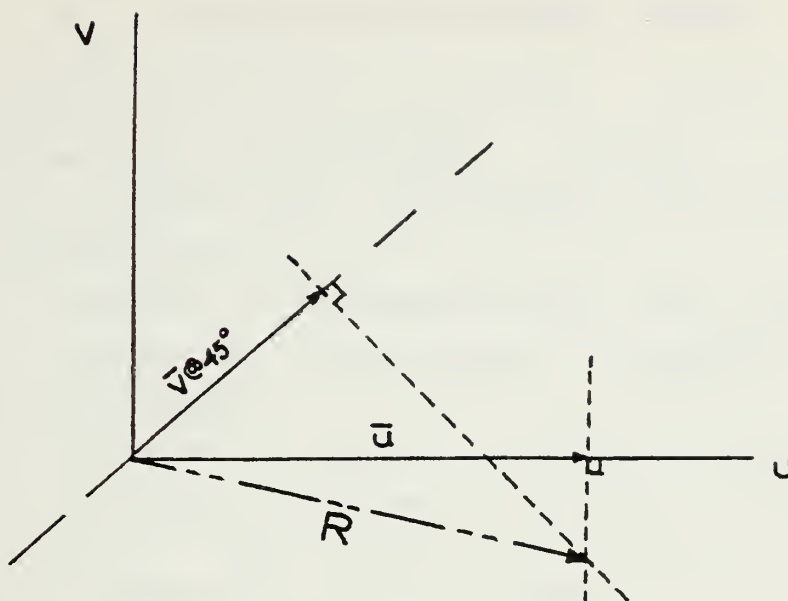


Zinc-hexachlororathane particles
(X5000 1cm = 2.0 μ m)

Figure 7

The final velocity component measured at each node was the result of averaging three successive readings from the velocimeter processor. Each of these readings represented the average of 4096 readings which had been validated to within 1.5% of the exact five-eighths validation count criteria.

The flow in the wind tunnel was stabilized at five inches per second to maintain a Reynolds number of about 40, which is in the realm of creeping flow. The experimental setup was designed to measure the steady flow about the cylinder, hence the relatively low Reynolds number, and no effort was made to obtain unsteady flow measurements. Three separate runs were conducted, two over the forward half of the control volume and one over the rear half. Because the beams of the laser anemometer were approximately one-sixteenth inch in diameter, several node position measurements were excluded due to inaccessibility. The majority of these were in close proximity to the cylinder. In order to obtain both an x- and a y-velocity component of the flow at every node which was accessible, two measurements were made, but because of the very small vertical component present in most of the flow, direct vertical beam pair measurement was unsuitable. Instead, after obtaining the horizontal component for each node in a run, a second series of measurements was made with the beam pairs inclined forty-five degrees from the vertical. In this fashion the y-component was determined by the following relationship:



It can be seen here that the unknown resultant (R) has a projection onto each axis representing the orientation of the beam pairs, thus the resultant is the vector which emanates from the origin and terminates at the intersection of the perpendiculars constructed from the \bar{u} and \bar{v} (at 45 degrees) vectors.

V. DESCRIPTION OF COMPUTER PROGRAM

The program found in the appendix has several comment cards inserted for clarification. However, a broader presentation is offered here. The program may be subdivided into four main sections:

Section 1: dimensioning and zeroing of parameters and arrays. (FLU00020 through FLU00690)

Section 2: input of node coordinates, system topology and known values of u , v , P , and right hand sides, and output of the same. (FLU00700 through FLU02090)

Section 3: computation of interpolation polynomials on an elemental level and arrangement into local element arrays. (FLU02100 through G000320)

Section 4: loading of the global influence matrix (TM) and solution of $(TM)(T)=(Q)$ by Gauss-Jordan partial pivoting and back substitution, with an iterative routine incorporated until convergence is attained, and associated print out. (FLU04470 through FLU04880)

The computer routine systematically tested the solution of field variables with the previous solution until all terms in the T and $T1$ arrays agreed within 0.001 (ESPILA). If the convergence test failed, the process was repeated from section 3.

Initially, the program was run on an IBM 360 in FORTRAN CLG mode, then an ensuing run was completed on the FORTRAN HCLG compiler and a time reduction of two-thirds was realized. The program, as given in the appendix, required approximately 375K bytes of core to compile and 675K bytes

to execute and output. Substantial space savings may be realized by utilizing banded matrix storage methods vice the method employed here, but due to time limitations this avenue was not fully explored.

The program attempts to solve simultaneously for all the field variables. However, introduction of zeros on the main diagonal of the TM influence matrix resulted in a singular matrix. Another approach was explored where the equation of continuity

$$\frac{\partial u}{\partial x} + \frac{\partial v}{\partial y} = 0$$

was replaced by

$$-\frac{1}{2}\nabla^2 P = \left[\frac{\partial v}{\partial x} \frac{\partial u}{\partial y} - \frac{\partial u}{\partial x} \frac{\partial v}{\partial y} \right]$$

and the resulting terms were added to the TM matrix and their respective right hand sides. The only field variables affected by this form of the continuity equation were the pressure variables, and depending on whether the local corner node involved in the local pressure equation was on the boundary or interior, different right hand sides had to be evaluated. This is the purpose of steps FLU04460 through GO00320. The simultaneous solution technique for all field variables applied to this new set of equations did not converge.

A third, unimplemented technique may be considered. Given the original matrix equations:

$$(1) \quad K_1 U + 0 + K_2 P = R_1$$

$$(2) \quad 0 + K_1 V + K_3 P = R_2$$

$$(3) \quad K_2 U + K_3 V + 0 = 0$$

Solution for u and v will result in

$$(1) \quad U = -K_1^{-1} K_2 P + K_1^{-1} R_1$$

$$(2) \quad V = -K_1^{-1} K_3 P + K_1^{-1} R_2$$

and multiplication by K_2 and K_3 yields

$$K_2 U = -K_2 K_1^{-1} K_3 P + K_2 K_1^{-1} R_1$$

$$K_3 V = -K_3 K_1^{-1} K_3 P + K_3 K_1^{-1} R_2$$

Summation of these equations allows substitution for the third matrix equation:

$$\left[K_2 K_1^{-1} K_3 + K_3 K_1^{-1} K_3 \right] P = K_2 K_1^{-1} R_1 + K_3 K_1^{-1} R_2$$

The matrix operating on P may be calculated on an algebraic level and entered, in terms of a_i , b_i and c_i , into the program in order to solve for the pressures at every corner node. The calculated P 's then would be entered into the field variable array and the partial pivoting routine, which involves only those terms where the field variable is not specified, would operate primarily on the first two matrix equations. In previous computer trials where all corner node pressures were specified, although not known to be correct, calculations were properly performed. This method would allow the actual pressures present in the control surface to be entered into the computer routine for further calculation of the velocity components.

VI. ANALYSIS OF RESULTS

No computer routine output was obtained for comparison of results, due to the inability of the program to converge. As such, comparison of the two methods cannot be offered here. The non-convergence of the program was investigated from several aspects: validity of the non-linear terms, correctness of the loading of the TM matrix on both the elemental and global levels, correctness of input, performance of the partial pivoting subroutines and the iteration scheme; all without success. In test cases the program initially solved for the unknowns within magnitude accuracy for a majority of terms. However, successive iterations resulted in oscillating solutions, even after twenty iterations. Convergence was expected after ten to fifteen iterations without under- or overrelaxation factors incorporated into the iteration scheme. After the new formulation of the continuity equation was incorporated into the computer routine, the program execution again resulted in a singular matrix when only the left and right hand and upper control surface boundaries had their respective pressures specified. Underflow occurred in the execution of the subroutine SOLVE at step SOL00260. Subsequent investigation revealed that the 178th and 179th rows of the reduced matrix equations were the cause of the underflow.

The data which were taken for runs number two and three are displayed in the appendix and are plotted on the finite element grid in Figure 8. Without the analytical results to compare the measured data only a qualitative statement may be made pertaining to the LDV output. It is readily seen that the trend of flow directions around the cylinder appears to be correct. By and large, the flow in close proximity to the cylinder was accelerated over the tcp and decelerated near the stagnation points. It is pointed out

here that the plot is a composite of two different trials, and as such, different free stream velocities were present for each run. In Figure 8 the vector representing the flow at a node was plotted and the magnitude of the vector in inches per second was displayed above the vector or by the node from which the velocity vector emanated.

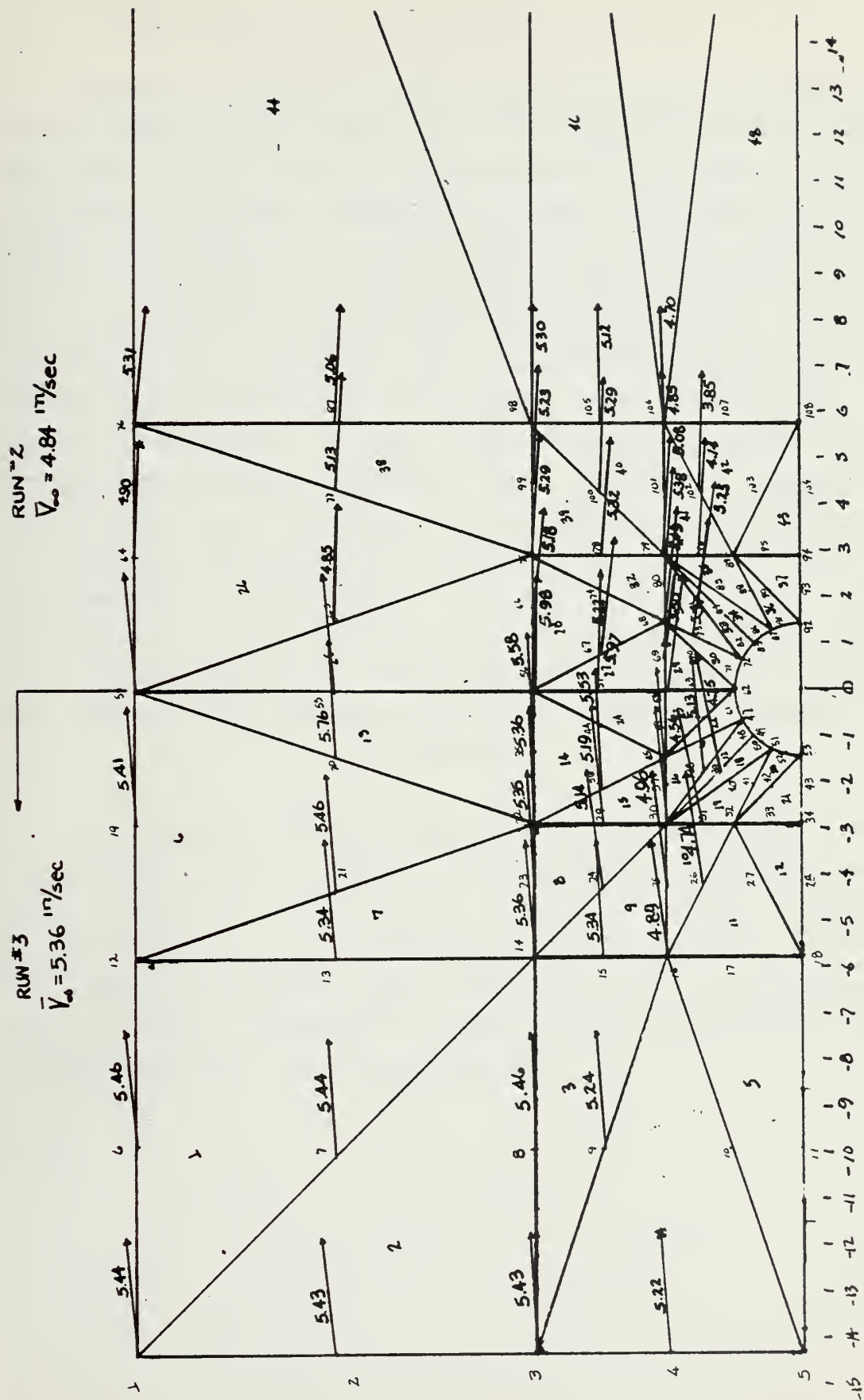


Figure 8

A. ERROR ANALYSIS

Re-positioning of the cylinder to its base location was accomplished with relatively low position error. Prior to each run the cylinder was aligned using the beam pairs as reference. In the horizontal mode, the beam pairs would strike the leading and trailing portions of the cylinder and reflect to positions horizontally opposed on the far side of the wind tunnel when correctly zeroed vertically. The same procedure was repeated for the vertical beam pair except position was checked by the upper beam reflecting to a vertical position on the far wall and the lower beam (at reduced intensity) striking the cylinder support on centerline. This procedure was repeated several times and the maximum deviation between any aligned positions was 0.2 millimeters horizontally or vertically. Thus, it was determined that the maximum positioning error inherent in the system would be the ratio of the smallest coordinate of any node measured and the aforementioned 0.2 millimeters or

$$0.2/3.75=0.5\%$$

Freestream velocity measurements were likewise tested for fluctuations. Typical measurement variations ranged from 0.129 to 0.142 (run number three; freestream measurements) in the horizontal mode and 0.0947 to 0.100 in the forty-five degree mode (velocities in meters/seconds). These figures represent a total of 10% variation which may be considered as $\pm 5\%$ from the mean.

VII. CONCLUSION

The experiment, as described, required approximately two to four hours for each run. aside from the initial alignment of the components and the cylinder, this was perhaps the greatest drawback of the system. Next, the exclusion of regions in close proximity to the cylinder from measurement was deemed to be a major factor in the small amount of data actually taken. The latter may be improved with a different experimental arrangement; particularly, the plexiglass section directly prefacing the optics transducer should be completely removed, thus allowing all angles of beam pair inclination, and in turn availing more locations to measurement. Another improvement which could be implemented would be unitization of the laser, transducer and photomultiplier tube arrangement. This would decrease the LDV's sensitivity to vibration and provide a more accurate optical axis alignment. The aforementioned improvements would still not decrease the time required for data collection, but the introduction of a two component system [Ref.4] would allow simultaneous measurement using orthogonal beam pairs. Furthermore, this type of system would not concern itself with the errors introduced in beam pair re-alignments performed with the single beam pair LDV.

The reproducibility of the experiment was judged to be good with the exception of exact duplication of the wind tunnel velocity between successive trials. This, of course, is primarily a function of the controllability of the tunnel motor and propellor assembly. It is estimated that with adequate facilities for incorporation of some of the aforementioned improvements, more accurate data may be obtained. The LDV displays great potential as a means of measuring a wide variety of dynamic fluid regimes accurately and without introduction of disturbance to the flow itself.

APPENDIX A

LDV DATA

RUN #2

Node	U(cm/sec)	V_{45° (cm/sec)	R(in/sec)	\angle°
64	12.43	8.43	4.90	-2.3
65	12.33	8.49	4.85	-1.5
66	13.10	8.33	5.18	-5.8
67	13.17	8.25	5.22	-6.5
68	13.87	8.72	5.49	-6.3
69	13.87	8.56	5.50	-7.2
73	14.03	8.58	5.57	-7.7
75	13.40	8.83	5.29	-3.9
76	13.43	8.62	5.31	-5.3
77	13.00	8.62	5.13	-3.6
78	13.47	8.87	5.32	-4.5
79	12.87	8.58	5.08	-3.3
80	13.63	8.91	5.38	-4.3
81	13.20	8.02	5.25	-8.0
96	10.50	6.94	4.14	-3.7
97	12.83	8.64	5.06	-2.7
98	13.47	9.54	5.30	0.1
99	13.27	8.92	5.23	-2.8
100	13.43	9.25	5.29	-1.5
101	12.33	8.83	4.85	0.7
102	9.77	6.69	3.85	-1.8
105	13.03	9.32	5.12	0.8
106	11.93	8.68	4.70	1.7

RUN #3

Node	U(cm/sec)	V@45°(cm/sec)	R(in/sec)	°
1	13.73	10.77	5.44	6.23
2	13.70	10.43	5.43	6.25
3	13.77	10.33	5.43	3.49
4	13.23	10.03	5.22	4.11
6	13.77	10.93	5.46	7.00
7	13.80	10.40	5.44	3.77
8	13.87	10.17	5.46	2.11
9	13.27	10.08	5.24	4.27
13	13.50	10.47	5.34	5.54
14	13.57	10.40	5.36	4.80
15	13.53	10.20	5.34	3.76
16	12.30	9.93	4.89	8.05
19	13.70	10.43	5.41	4.38
20	14.60	10.87	5.76	3.02
21	13.83	10.57	5.46	4.63
22	13.60	10.06	5.36	2.65
23	13.57	10.23	5.35	3.79
24	12.93	10.40	5.14	7.84
25	12.50	9.92	4.96	7.00
26	11.90	9.64	4.74	8.27
29	13.13	10.16	5.19	5.40
30	12.57	9.80	4.98	5.86
31	11.30	9.76	4.56	12.50
35	14.17	10.47	5.58	2.60
36	14.03	10.43	5.53	4.36
37	13.23	10.07	5.22	4.36
38	12.97	10.09	5.13	5.72
39	11.83	10.03	4.75	11.24
54	14.03	10.87	5.55	5.58
55	14.17	11.03	5.61	5.76
56	15.20	10.57	5.98	-0.90
57	15.17	10.47	5.97	-1.36
58	16.27	10.00	6.46	-7.46
59	14.37	10.20	5.66	0.20


```

C      READ IN NUMBER OF NODES AND ELEMENTS AND NO. CORNER NODES
C      READ(NREAD,1005)NN,NE,NNCN
C
C      INITIALIZE ALL PARAMETERS

```

```

      MM=NN+NN+NNCN

```

```

      DC 50 I=1,120

```

```

      XC(I)=0.

```

```

      YC(I)=0.

```

```

      NVS(I)=0

```

```

      NCP(I)=0

```

```

      NPS(I)=0

```

```

      NCS(I)=0

```

```

      50 CONTINUE

```

```

      DO 51 I=1,MM

```

```

      NVIS(I)=0

```

```

      NQIS(I)=0

```

```

      T(I)=0.

```

```

      Q(I)=0.

```

```

      Z(I)=0.

```

```

      C(I)=0.

```

```

      DO 51 J=1,MM

```

```

      B(I,J)=0.

```

```

      51 CONTINUE

```

```

      DO 53 I=1,15

```

```

      N(I)=0

```

```

      DO 53 J=1,15

```

```

      TM$(I,J)=0.

```

```

      53 CONTINUE

```

```

      DO 54 I=1,6

```

```

      RP$(I)=0.

```

```

      ZP$(I)=0.

```

```

      U(I)=0.0

```

```

      V(I)=0.0

```

```

      DO 54 K=1,6

```

```

      QZ1(I,K)=0.0

```

```

      QZB(I)=0.0

```

```

      QZC(I)=0.0

```

```

      QZ2(I,K)=0.0

```

```

      QZ3(I,K)=0.0

```

```

      54 CONTINUE

```

```

      DO 55 I=1,3

```

```

      XC$(I)=0.

```

```

      YC$(I)=0.

```

```

      NT(I)=0

```

```

      55 CONTINUE

```

```

FLU00390
FLU00400
FLU00410
FLU00420
FLU00430
FLU00440

FIX00020
FIX00030
FIX00040
FIX00050
FIX00070
FIX00080
FIX00200
FIX00090
FIX00100
FIX00060
FIX00210
FIX00110
FIX00120
FIX00130
FIX00140
FIX00150
FIX00160
FIX00170
FIX00180
FIX00230
FIX00240
FIX00250
FIX00260
FIX00270

FIX00290
FIX00300

```

```

FIX00310
FIX00320
FIX00330
FIX00340

FIX00350

```



```

DO 56 I=1,4
  NLCY(I)=0.0
  NRCY(I)=0.0
56 CONTINUE
C READ NODE NUMBERS AND COORDINATES
C
DO 100 J=1,NN
  READ(NREAD,1006)WORD,I,XC(I),YC(I)
  IF (WORD.EQ.STOP) GO TO 101
  NCN(J)=I
100 CONTINUE
101 NNCN=J-1
C
C THE ARRAY NCP(J) GENERATES THE GLOBAL PRESSURE INDICES (P1,P2.)
C THUS PRESSURE NODES ARE LABELED AS CORNER NODES ARE INPUTED
C WHEN ONE INPUTS A GLOBAL CORNER NODE FOR J
C
DO 107 J=1,NNCN
  NCP(NCN(J)) =J+NN+NN
107 CONTINUE
C
C SYSTEM TOPOLOGY( ELEMENT NO. AND NODE NUMBERS IN
C COUNTER-CLOCKWISE FASHION STARTING AT ANY CORNER NODE
C ALWAYS COUNT FROM UPPER LEFT HAND CORNER
C
DO 105 I=1,NE
  READ(NREAD,1010)J,NODE(J,1),NODE(J,2),NODE(J,3),
  1 NODE(J,4),NODE(J,5),NODE(J,6)
105 CONTINUE
  MAXDIF=0
  DO 108 I=1,NE
    DO 108 J=1,6
      DO 108 K=1,6
        LL=IABS(NODE(I,J)-NODE(I,K))
        IF(LL.GT.MAXDIF) MAXDIF=LL
      IBAND=2*(MAXDIF+1)
      NEQ=2*NN+NNCN
108 CONTINUE
107 WRITE(NWRITE,1017)IBAND,NEQ
1017 FORMAT(5X,'IBAND=',I3,'/',5X,'NEQ =',I3,'/')
C READ NODES WHERE BOTH U AND V VELOCITY IS SPECIFIED
C
DO 110 I=1,MM
  READ(NREAD,1006)WORD,NVELS,VELU,VELV
  IF(WORD.EQ.STOP) GO TO 111
  NVS(I)=NVELS
  T(NVS(I))=VELU
  T(NVS(I)+1)=VELV
110 CONTINUE
111 CONTINUE

```

FLU00690
 FLU00700
 FLU00710
 FLU00720
 FLU00730
 FLU00740
 FLU00750
 FLU00760
 FLU00770
 FLU00780
 FLU00790
 FLU00800
 FLU00810
 FLU00820
 FLU00830
 FLU00840
 FLU00850
 FLU00860
 FLU00870
 FLU00880
 FLU00890
 FLU00900
 FLU00910
 FLU00920
 FLU00930
 FLU00940
 FLU00950
 FLU00960
 FLU00970
 FLU00980
 FLU00990
 FLU01000
 FLU01010
 FLU01020
 FLU01030
 FLU01040
 FLU01050
 FLU01060
 FLU01070
 FLU01080
 FLU01090
 FLU01100
 FLU01110
 FLU01120


```

110 T(NVS(I)+NN)=VELV
    CONTINUE
C COUNT NODES HAVING SPECIFIED VELOCITIES
C
111 NNVELS= I-1
C
C READ QX AND QY VALUES AT INTERNAL NODES
DO 125 I=1,NN
  READ(NREAD,1006)WORD,NQXY,QXNS,QYNS
  IF(WORD.EQ.STOP) GO TO 126
  NQS(I)=NQXY
  Q(NQS(I))=QXNS*PRES
  Q(NQS(I)+NN)=QYNS*PRES
125 CONTINUE
126 NNQXY=I-1
C
C READ NODE NUMBERS AND PRESSURE WHEREE PRESSURE IS SPECIFIED
C
DO 130 I=1,NN
  READ(NREAD,1025)WORD,NP,PNP
  IF(WORD.EQ.STOP)GO TO 135
  NPS(I)=NP
  T(NCP(NPS(I)))=PNP
130 CONTINUE
C COUNT BOUNDARY NODES WHERE PRESSURE SPECIFIED
C
135 NNPS= I-1
C
C READ PRESSURE NODES WHERE Q IS SPECIFIED
C
DO 141 I=1,MM
  READ(NREAD,1025)WORD,NPQ,QNPQ
  IF(WORD.EQ.STOP)GO TO 142
  NPS(I+NNPS)=NPQ
  Q(NCP(NPS(I+NNPS)))=QNPQ
141 CONTINUE
142 NNPQ=I-1
C
C READ IN CORNER NODES WHICH ARE CONTAINED IN THE INTERIOR
C
DO 143 I=1,MM
  READ(NREAD,7654) NINT

```

FLU01130
 FLU01140
 FLU01150
 FLU01160
 FLU01170
 FLU01180
 FLU01190
 FLU01200
 FLU01210
 FLU01220
 FLU01230
 FLU01240
 FLU01250
 FLU01260

FLU01290
 FLU01300
 FLU01310
 FLU01320
 FLU01330
 FLU01340
 FLU01350
 FLU01360
 FLU01370
 FLU01380
 FLU01390
 FLU01400
 FLU01410
 FLU01420
 FLU01430
 PRE00100
 PRE00090

PRE00110
 PRE00130
 PRE00010
 PRE00020
 PRE00030
 PRE00040
 PRE00050
 PRE00070
 PRE00080
 QZ 00160

QZ 00140
 QZ 00070
 QZ 00080


```

IF (WORD.EQ.STOP) GO TO 147
NI(I)=NINT
143 CONTINUE
7654 FORMAT(6X,A4,14I4)
147 CONTINUE
C
C NCIS IS A LIST OF THE INDICES OF KNOWN QX QY
C
      DO 1140 I=1,NNQXY
        NQIS(I)=NQS(I)
        NQIS(I+NNQXY)=NQS(I)+NN
1140 CONTINUE
      DO 1142 I=1,NNPQ
        NQIS(I+2*NNQXY)=NPS(I+NNPS)+2*NN
1142 CONTINUE
C
C NVIS IS A LIST OF INDICIES OF KNOWN VELOCITIES AND PRESSURES
C
      DO 1150 I=1,NNVELS
        NVIS(I)=NVS(I)
        NVIS(I+NNVELS)=NVS(I)+NN
1150 CONTINUE
      DO 1160 J=1,NNPS
        NVIS(2*NNVELS+J)=NCP(NPS(J))
1160 CONTINUE
C
C NTOTQ TOTAL NUMBER OF KNOWN QX AND QY
C
      NTOTQ=2*NNQXY +NNPQ
      NTOTVP=2*NNVELS+NNPS
C
C PRINT ALL INPUT DATA
C
      WRITE(NWRITE,1035)NN,NE,NNCN
      WRITE(NWRITE,1040)
      DO 150 I=1,NNCN
        WRITE(NWRITE,1045)NCN(I),XC(NCN(I)),YC(NCN(I))
        CONTINUE
150 WRITE(NWRITE,1050)
      DO 155 I=1,NE
        WRITE(NWRITE,1055)I,NODE(I,1),NODE(I,2),NODE(I,3),
          1 NODE(I,4),NODE(I,5),NODE(I,6)
155 CONTINUE
      WRITE(NWRITE,1060)
      DO 160 I=1,NNVELS
        WRITE(NWRITE,1065)I,NVS(I),T(NVS(I)),T(NVS(I)+NN)
160 CONTINUE
      WRITE(NWRITE,1070)

```

QZ 00100
8Z 00 10

FLU01440
FLU01450
FLU01460
FLU01470
FLU01480
FLU01490
FLU01500

FLU01510
FLU01530
FLU01540
FLU01550
FLU01560
FLU01570
FLU01580
FLU01590
FLU01600
FLU01610
FLU01620
FLU01630
FLU01640

FLU01710
FLU01720
FLU01730
FLU01740
FLU01750
FLU01760
FLU01770
FLU01780
FLU01790
FLU01800
FLU01810
FLU01820
FLU01830
FLU01840
FLU01850
FLU01860
FLU01870
FLU01880


```

DO 165 I=1,NNQXY
WRITE(NWRITE,1065)I,NQS(I),Q(NQS(I)),Q(NQS(I)+NN)
CONTINUE
165 IF(NNPQ.EQ.0)GO TO 163
WRITE(NWRITE,1071)
DO 163 I=1,NNPQ
WRITE(NWRITE,1072)I,NPS(I+NNPS),Q(NCP(NPS(I+NNPS)))
163 CONTINUE
WRITE(NWRITE,1080)
DO 170 I=1,NNPS
WRITE(NWRITE,1085)I,NPS(I),T(NCP(NPS(I)))
170 CONTINUE
177 CONTINUE
DO 179 I=1,MM
RHS(I)=0.0
DO 179 J=1,MM
TM(I,J)=0.0
175 CONTINUE
C
C END OF INPUT AND VERIFICATION ROUTINE
C
DO 300 K=1,NE
N1=NODE(K,1)
N2=NODE(K,2)
N3=NODE(K,3)
N4=NODE(K,4)
N5=NODE(K,5)
N6=NODE(K,6)
N7 = NODE(K,1)+NN
N8 = NODE(K,2)+NN
N9 = NODE(K,3)+NN
N10=NODE(K,4)+NN
N11=NODE(K,5)+NN
N12=NODE(K,6)+NN
N13=NCP(NODE(K,1))
N14=NCP(NODE(K,3))
N15=NCP(NODE(K,5))
XC$(1)=XC(NODE(K,1))
XC$(2)=XC(NODE(K,3))
XC$(3)=XC(NODE(K,5))
YC$(1)=YC(NODE(K,1))
YC$(2)=YC(NODE(K,3))
YC$(3)=YC(NODE(K,5))
A=.0229248
AA=1.
A1=XC$(2)*YC$(3)-XC$(3)*YC$(2)
A2=XC$(3)*YC$(1)-XC$(1)*YC$(3)
A3=XC$(1)*YC$(2)-XC$(2)*YC$(1)

```

```

FLU01890
FLU01900
FLU01910
PRE00160
PRE00170
PRE00180
PRE00190
FLU01920
FLU01930
FLU01940
FLU01950
FLU02030
FLU02040
FLU02050
FLU02060
FLU02070
FLU02080
FLU02090
FLU02100
FLU02110
FLU02120
FLU02130
FLU02140
FLU02150
FLU02160
FLU02170
FLU02180
FLU02190
FLU02200
FLU02210
FLU02220
FLU02230
FLU02240
FLU02250
FLU02260
FLU02270
FLU02280
FLU02290
FLU02300
FLU02310
FLU02320
FLU02340
FLU02350
FLU02360
FLU02370

```



```

B1=YC$(2)-YC$(3)
B2=YC$(3)-YC$(1)
B3=YC$(1)-YC$(2)
C1=XC$(3)-XC$(2)
C2=XC$(1)-XC$(3)
C3=XC$(2)-XC$(1)
DEL=ABS(0.5*(YC$(1)-YC$(2)))*AA
1 3*(YC$(1)-YC$(2))*AA
CONST=(1.*A/(3.*DEL))*AA
D1=-B1/6.
D2=-B2/6.
D3=-B3/6.
E1=-C1/6.
E2=-C2/6.
E3=-C3/6.
F1=B1/2520.
F2=B2/2520.
F3=B3/2520.
G1=C1/2520.
G2=C2/2520.
G3=C3/2520.
U1=T1(N1)
U2=T1(N2)
U3=T1(N3)
U4=T1(N4)
U5=T1(N5)
U6=T1(N6)
V1=T1(N7)
V2=T1(N8)
V3=T1(N9)
V4=T1(N10)
V5=T1(N11)
V6=T1(N12)
TM$(1,1)=.75*(B1*B1+C1*C1)*CONST
TM$(1,2)=(B1*B2+C1*C2)*CONST
TM$(1,3)=-TM$(1,2)*.25
TM$(1,4)=0.
TM$(1,6)=(B1*B3+C1*C3)*CONST
TM$(1,5)=-TM$(1,6)*.25
TM$(3,3)=.75*(B2*B2+C2*C2)*CONST
TM$(3,4)=(B2*B3+C2*C3)*CONST
TM$(3,5)=-TM$(3,4)*.25
TM$(1,2)=TM$(1,2)
TM$(2,1)=TM$(1,2)
TM$(2,3)=TM$(1,2)
TM$(2,2)=8./3.*{TM$(1,1)+TM$(3,3))+2.*TM$(1,2)
TM$(2,4)=2.*TM$(1,6)+TM$(3,4)+TM$(1,2)+4./3.*TM$(3,3)
TM$(2,5)=0.
TM$(2,6)=TM$(1,6)+2.*TM$(3,4)+TM$(1,2)+4./3.*TM$(1,1)

```

```

FLU02380
FLU02390
FLU02400
FLU02410
FLU02420
FLU02430
FLU02440
FLU02450
FLU02460
FLU02470
FLU02480
FLU02490
FLU02500
FLU02510
FLU02520
FI X00010
FI X00020
FI X00030
FI X00040
FI X00050
FI X00060
FI X00080
FI X00090
FI X00100
FI X00110
FI X00120
FI X00130
FI X00140
FI X00150
FI X00160
FI X00170
FI X00180
FI X00190
FLU02590
FLU02600
FLU02610
FLU02620
FLU02630
FLU02640
FLU02650
FLU02660
FLU02670
FLU02680
FLU02690
FLU02700
FLU02710
FLU02720
FLU02730

```



```

TM$(3,1)=TM$(1,3)
TM$(3,2)=TM$(2,3)
TM$(3,6)=0.
      TM$(5,5)=.75 *(B3*B3+C3*C3)*CONST
TM$(4,1)=TM$(1,4)
TM$(4,2)=TM$(2,4)
TM$(4,3)=TM$(3,4)
TM$(4,4)=8./3*(TM$(3,3)+TM$(5,5))+2.*TM$(3,4)
TM$(4,5)=TM$(3,4)
TM$(4,6)=TM$(1,6)+TM$(3,4)+2.*TM$(1,2)+4./3.*TM$(5,5)
TM$(6,3)=TM$(3,6)
TM$(5,1)=TM$(1,5)
TM$(5,2)=TM$(2,5)
TM$(5,3)=TM$(3,5)
TM$(5,4)=TM$(4,5)
TM$(5,6)=TM$(1,6)
TM$(6,1)=TM$(1,6)
TM$(6,2)=TM$(2,6)
TM$(6,4)=TM$(4,6)
TM$(6,5)=TM$(5,6)
TM$(6,6)=8./3*(TM$(5,5)+TM$(1,1))+2.*TM$(1,6)
      IF(NCASE.NE.1)GO TO 3000

```

```

FLU02740
FLU02750
FLU02760
FLU02770
FLU02780
FLU02790
FLU02800
FLU02810
FLU02820
FLU02830
FLU02840
FLU02850
FLU02860
FLU02870
FLU02880
FLU02890
FLU02900
FLU02910
FLU02920
FLU02930
FLU02940
FLU02950

```

CCCCC

BEGIN INPUT OF NON-LINEAR TERMS

```

1 TM$(1,1)=TM$(1,1)-
  (F1*(78.*U1+48.*U2+(-9.*U3)+12.*U4+(-9.*U5)+48.*U6))
1 TM$(1,2)=TM$(1,2)-
  (F2*(120.*U1+48.*U2-16.*U3-16.*U4-16.*U5+48.*U6))-
2 (F1*(24.*U1-32.*U2-16.*U3-48.*U4+4.*U5-16.*U6))
1 TM$(1,3)=TM$(1,3)-
  (F2*(-18.*U1-32.*U2-9.*U3-20.*U4+11.*U5-16.*U6))
1 TM$(1,4)=TM$(1,4)-
  (F3*(24.*U1-32.*U2-16.*U3-48.*U4+4.*U5-16.*U6))-
2 (F2*(24.*U1-16.*U2+4.*U3-48.*U4-16.*U5-32.*U6))
1 TM$(1,5)=TM$(1,5)-
  (F3*(-18.*U1-16.*U2+11.*U3-20.*U4-9.*U5-32.*U6))
1 TM$(1,6)=TM$(1,6)-
  (F3*(120.*U1+48.*U2-16.*U3-16.*U4-16.*U5+48.*U6))-
2 (F1*(24.*U1-16.*U2+4.*U3-48.*U4-16.*U5-32.*U6))
1 TM$(2,1)=TM$(2,1)-
  (F1*(48.*U1+160.*U2-32.*U3+16.*U4-20.*U5+80.*U6))
1 TM$(2,2)=TM$(2,2)-
  (F2*(48.*U1+384.*U2-32.*U3+128.*U4-48.*U5+192.*U6))-
2 (F1*(-32.*U1+384.*U2+48.*U3+192.*U4-48.*U5+128.*U6))
1 TM$(2,3)=TM$(2,3)-

```

```

FIX00190
FIX00200
FIX00210
FIX00220
FIX00230
FIX00240
FIX00250
FIX00260
FIX00270
FIX00280
FIX00290
FIX00300
FIX00310
FIX00320
FIX00330
FIX00340
FIX00350
FIX00370
FIX00380
FIX00390
FIX00400

```


1 (F2*(-32.*U1+160.*U2+48.*U3+80.*U4-20.*U5+16.*U6))
TM\$(2,4)=TM\$(2,4)
1 (F3*(-32.*U1+384.*U2+48.*U3+192.*U4-48.*U5+128.*U6))-
2 (F2*(-16.*U1+128.*U2-16.*U3+128.*U4-16.*U5+128.*U6))
TM\$(2,5)=TM\$(2,5)
1 (F3*(-16.*U1-96.*U2-16.*U3+16.*U4+12.*U5+16.*U6))
TM\$(2,6)=TM\$(2,6)
1 (F3*(48.*U1+384.*U2-32.*U3+128.*U4-48.*U5+192.*U6))-
2 (F1*(-16.*U1+128.*U2-16.*U3+128.*U4-16.*U5+128.*U6))
TM\$(3,1)=TM\$(3,1)
1 (F1*(-9.*U1-32.*U2-18.*U3-16.*U4+11.*U5-20.*U6))
TM\$(3,2)=TM\$(3,2)
1 (F2*(-16.*U1-32.*U2+24.*U3-16.*U4+4.*U5-48.*U6))-
2 (F1*(-16.*U1+48.*U2+120.*U3+48.*U4-16.*U5-16.*U6))
TM\$(3,3)=TM\$(3,3)
1 (F2*(-9.*U1+48.*U2+78.*U3+48.*U4-9.*U5+12.*U6))
TM\$(3,4)=TM\$(3,4)
1 (F3*(-16.*U1+48.*U2+120.*U3+48.*U4-16.*U5-16.*U6))-
2 (F2*(4.*U1-16.*U2+24.*U3-32.*U4-16.*U5-48.*U6))
TM\$(3,5)=TM\$(3,5)
1 (F3*(11.*U1-16.*U2-18.*U3-32.*U4-9.*U5-20.*U6))
TM\$(3,6)=TM\$(3,6)
1 (F3*(-16.*U1-32.*U2+24.*U3-16.*U4+4.*U5-48.*U6))-
2 (F1*(4.*U1-16.*U2+24.*U3-32.*U4-16.*U5-48.*U6))
TM\$(4,1)=TM\$(4,1)
1 (F1*(12.*U1+16.*U2-16.*U3-96.*U4-16.*U5+16.*U6))
TM\$(4,2)=TM\$(4,2)
1 (F2*(-16.*U1+128.*U2-16.*U3+128.*U4-16.*U5+128.*U6))-
2 (F1*(-48.*U1+192.*U2+48.*U3+384.*U4-32.*U5+128.*U6))
TM\$(4,3)=TM\$(4,3)
1 (F2*(-20.*U1+80.*U2+48.*U3+160.*U4-32.*U5+16.*U6))
TM\$(4,4)=TM\$(4,4)
1 (F3*(-48.*U1+192.*U2+48.*U3+384.*U4-32.*U5+128.*U6))-
2 (F2*(-48.*U1+128.*U2-32.*U3+384.*U4+48.*U5+192.*U6))
TM\$(4,5)=TM\$(4,5)
1 (F3*(-20.*U1+16.*U2-32.*U3+160.*U4+48.*U5+80.*U6))
TM\$(4,6)=TM\$(4,6)
1 (F3*(-16.*U1+128.*U2-16.*U3+128.*U4-16.*U5+128.*U6))-
2 (F1*(-48.*U1+128.*U2-32.*U3+384.*U4+48.*U5+192.*U6))
TM\$(5,1)=TM\$(5,1)
1 (F1*(5,1)=TM\$(5,1))
1 (F1*(-9.*U1-20.*U2+11.*U3-16.*U4-18.*U5-32.*U6))
TM\$(5,2)=TM\$(5,2)
1 (F2*(-16.*U1-48.*U2+4.*U3-16.*U4+24.*U5-32.*U6))-
2 (F1*(4.*U1-48.*U2-16.*U3-32.*U4+24.*U5-16.*U6))
TM\$(5,3)=TM\$(5,3)
1 (F2*(11.*U1-20.*U2-9.*U3-32.*U4-18.*U5-16.*U6))
TM\$(5,4)=TM\$(5,4)
1 (F3*(4.*U1-48.*U2-16.*U3-32.*U4+24.*U5-16.*U6))-

FI X00410
FI X00420
FI X00430
FI X00440
FI X00450
FI X00460
FI X00470
FI X00480
FI X00490
FI X00500
FI X00510
FI X00520
FI X00530
FI X00540
FI X00550
FI X00560
FI X00570
FI X00580
FI X00590
FI X00600
FI X00610
FI X00620
FI X00630
FI X00640
FI X00650
FI X00660
FI X00670
FI X00690
FI X00700
FI X00710
FI X00720
FI X00730
FI X00740
FI X00750
FI X00760
FI X00770
FI X00780
FI X00790
FI X00800
FI X00810
FI X00820
FI X00830
FI X00840
FI X00850
FI X00860
FI X00870
FI X00880

2 (F2*(-16.*U1-16.*U2-16.*U3+48.*U4+120.*U5+48.*U6))
 TM\$(5,5)=TM\$(5,5)-
 1 (F3*(-9.*U1+12.*U2-9.*U3+48.*U4+78.*U5+48.*U6))
 TM\$(5,6)=TM\$(5,6)-
 1 (F3*(-16.*U1-48.*U2+4.*U3-16.*U4+24.*U5-32.*U6))-
 2 (F1*(-16.*U1-16.*U2-16.*U3+48.*U4+120.*U5+48.*U6))
 TM\$(6,1)=TM\$(6,1)-
 1 (F1*(48.*U1+80.*U2-20.*U3+16.*U4-32.*U5+160.*U6))
 TM\$(6,2)=TM\$(6,2)-
 1 (F2*(48.*U1+192.*U2-48.*U3+128.*U4-32.*U5+384.*U6))-
 2 (F1*(-16.*U1+128.*U2-16.*U3+128.*U4-16.*U5+128.*U6))
 TM\$(6,3)=TM\$(6,3)-
 1 (F2*(-16.*U1+16.*U2+12.*U3+16.*U4-16.*U5-96.*U6))
 TM\$(6,4)=TM\$(6,4)-
 1 (F2*(-16.*U1+128.*U2-16.*U3+128.*U4-16.*U5+128.*U6))-
 2 (F3*(-32.*U1+128.*U2-48.*U3+192.*U4+48.*U5+384.*U6))
 TM\$(6,5)=TM\$(6,5)-
 1 (F3*(-32.*U1+16.*U2-20.*U3+80.*U4+48.*U5+160.*U6))
 TM\$(6,6)=TM\$(6,6)-
 1 (F3*(48.*U1+192.*U2-48.*U3+128.*U4-32.*U5+384.*U6))-
 2 (F1*(-32.*U1+128.*U2-48.*U3+192.*U4+48.*U5+384.*U6))
 TM\$(1,1)=TM\$(1,1)-
 1 (G1*(78.*V1+48.*V2+(-9.*V3)+12.*V4+(-9.*V5)+48.*V6))
 TM\$(1,2)=TM\$(1,2)-
 1 (G2*(120.*V1+48.*V2-16.*V3-16.*V4-16.*V5+48.*V6))-
 2 (G1*(24.*V1-32.*V2-16.*V3-48.*V4+4.*V5-16.*V6))
 TM\$(1,3)=TM\$(1,3)-
 1 (G2*(-18.*V1-32.*V2-9.*V3-20.*V4+11.*V5-16.*V6))
 TM\$(1,4)=TM\$(1,4)-
 1 (G3*(24.*V1-32.*V2-16.*V3-48.*V4+4.*V5-16.*V6))-
 2 (G2*(24.*V1-16.*V2+4.*V3-48.*V4-16.*V5-32.*V6))
 TM\$(1,5)=TM\$(1,5)-
 1 (G3*(-18.*V1-16.*V2+11.*V3-20.*V4-9.*V5-32.*V6))
 TM\$(1,6)=TM\$(1,6)-
 1 (G3*(120.*V1+48.*V2-16.*V3-16.*V4-16.*V5+48.*V6))-
 2 (G1*(24.*V1-16.*V2+4.*V3-48.*V4-16.*V5-32.*V6))
 TM\$(2,1)=TM\$(2,1)-
 1 (G1*(48.*V1+160.*V2-32.*V3+16.*V4-20.*V5+80.*V6))
 TM\$(2,2)=TM\$(2,2)-
 1 (G2*(48.*V1+384.*V2-32.*V3+128.*V4-48.*V5+192.*V6))-
 2 (G1*(-32.*V1+384.*V2+48.*V3+192.*V4-48.*V5+128.*V6))
 TM\$(2,3)=TM\$(2,3)-
 1 (G2*(-32.*V1+160.*V2+48.*V3+80.*V4-20.*V5+16.*V6))
 TM\$(2,4)=TM\$(2,4)-
 1 (G3*(-32.*V1+384.*V2+48.*V3+192.*V4-48.*V5+128.*V6))-

F1X00890
 F1X00900
 F9X00 0
 F1X00920
 F1X00930
 F1X00940
 F1X00950
 F1X00960
 F1X00970
 F1X00980
 F1X00990
 F1X01000
 F1X01010
 F1X01020
 F1X01030
 F1X01040
 F1X01050
 F1X01060
 F1X01070
 F1X01080
 F1X01090
 F1X01100
 F1X01110
 F1X00200
 F1X00210
 F1X00220
 F1X00230
 F1X00240
 F1X00250
 F1X00260
 F1X00270
 F1X00280
 F1X00290
 F1X00300
 F1X00310
 F1X00320
 F1X00330
 F1X00340
 F1X00350
 F1X00360
 F1X00370
 F1X00380
 F1X00390
 F1X00400
 F1X00410
 F1X00420
 F1X00430
 F1X00440

2(G2*(-16.*V1+128.*V2-16.*V3+128.*V4-16.*V5+128.*V6))
 TM\$(2,5)=-TM\$(2,5)-
 1(G3*(-16.*V1-96.*V2-16.*V3+16.*V4+12.*V5+16.*V6))
 TM\$(2,6)=-TM\$(2,6)-
 1(G3*(-48.*V1+384.*V2-32.*V3+128.*V4-48.*V5+192.*V6))-
 2(G1*(-16.*V1+128.*V2-16.*V3+128.*V4-16.*V5+128.*V6))
 TM\$(3,1)=-TM\$(3,1)-
 1(G1*(-9.*V1-32.*V2-18.*V3-16.*V4+11.*V5-20.*V6))
 TM\$(3,2)=-TM\$(3,2)-
 1(G2*(-16.*V1-32.*V2+24.*V3-16.*V4+4.*V5-48.*V6))-
 2(G1*(-16.*V1+48.*V2+120.*V3+48.*V4-16.*V5-16.*V6))
 TM\$(3,3)=-TM\$(3,3)-
 1(G2*(-9.*V1+48.*V2+78.*V3+48.*V4-9.*V5+12.*V6))
 TM\$(3,4)=-TM\$(3,4)-
 1(G3*(-16.*V1+48.*V2+120.*V3+48.*V4-16.*V5-16.*V6))-
 2(G2*(-4.*V1-16.*V2+24.*V3-32.*V4-16.*V5-48.*V6))
 TM\$(3,5)=-TM\$(3,5)-
 1(G3*(-11.*V1-16.*V2-18.*V3-32.*V4-9.*V5-20.*V6))
 TM\$(3,6)=-TM\$(3,6)-
 1(G3*(-16.*V1-32.*V2+24.*V3-16.*V4+4.*V5-48.*V6))-
 2(G1*(-4.*V1-16.*V2+24.*V3-32.*V4-16.*V5-48.*V6))
 TM\$(4,1)=-TM\$(4,1)-
 1(G1*(-12.*V1+16.*V2-16.*V3-96.*V4-16.*V5+16.*V6))
 TM\$(4,2)=-TM\$(4,2)-
 1(G2*(-16.*V1+128.*V2-16.*V3+128.*V4-16.*V5+128.*V6))-
 2(G1*(-48.*V1+192.*V2+48.*V3+384.*V4-32.*V5+128.*V6))
 TM\$(4,3)=-TM\$(4,3)-
 1(G2*(-20.*V1+80.*V2+48.*V3+160.*V4-32.*V5+16.*V6))
 TM\$(4,4)=-TM\$(4,4)-
 1(G3*(-48.*V1+192.*V2+48.*V3+384.*V4-32.*V5+128.*V6))-
 2(G2*(-48.*V1+128.*V2-32.*V3+384.*V4+48.*V5+192.*V6))
 TM\$(4,5)=-TM\$(4,5)-
 1(G3*(-20.*V1+16.*V2-32.*V3+160.*V4+48.*V5+80.*V6))
 TM\$(4,6)=-TM\$(4,6)-
 1(G3*(-16.*V1+128.*V2-16.*V3+128.*V4-16.*V5+128.*V6))-
 2(G1*(-48.*V1+128.*V2-32.*V3+384.*V4+48.*V5+192.*V6))
 TM\$(5,1)=-TM\$(5,1)-
 1(G1*(-9.*V1-20.*V2+11.*V3-16.*V4-18.*V5-32.*V6))
 TM\$(5,2)=-TM\$(5,2)-
 1(G2*(-16.*V1-48.*V2+4.*V3-16.*V4+24.*V5-32.*V6))-
 2(G1*(-4.*V1-48.*V2-16.*V3-32.*V4+24.*V5-16.*V6))
 TM\$(5,3)=-TM\$(5,3)-
 1(G2*(-11.*V1-20.*V2-9.*V3-32.*V4-18.*V5-16.*V6))
 TM\$(5,4)=-TM\$(5,4)-
 1(G3*(-4.*V1-48.*V2-16.*V3-32.*V4+24.*V5-16.*V6))-
 2(G2*(-16.*V1-16.*V2-16.*V3+48.*V4+120.*V5+48.*V6))
 TM\$(5,5)=-TM\$(5,5)-
 1(G3*(-9.*V1+12.*V2-9.*V3+48.*V4+78.*V5+48.*V6))

F1X00450
 F1X00460
 F1X00470
 F1X00480
 F1X00490
 F1X00500
 F1X00510
 F1X00520
 F1X00530
 F1X00540
 F1X00550
 F1X00560
 F1X00570
 F1X00580
 F1X00590
 F1X00600
 F1X00610
 F1X00620
 F1X00630
 F1X00640
 F1X00650
 F1X00660
 F1X00670
 F1X00680
 F1X00690
 F1X00700
 F1X00710
 F1X00720
 F1X00730
 F1X00740
 F1X00750
 F1X00760
 F1X00770
 F1X00780
 F1X00790
 F1X00800
 F1X00810
 F1X00820
 F1X00830
 F1X00840
 F1X00850
 F1X00860
 F1X00870
 F1X00880
 F1X00890
 F1X00900
 F1X00910
 F1X00920

TM\$(11,11,10)=TM\$(5,2)
 TM\$(11,11,9)=TM\$(5,3)
 TM\$(11,11,8)=TM\$(5,4)
 TM\$(11,11,7)=TM\$(5,5)
 TM\$(11,11,6)=TM\$(5,6)
 TM\$(11,11,5)=TM\$(6,1)
 TM\$(11,11,4)=TM\$(6,2)
 TM\$(11,11,3)=TM\$(6,3)
 TM\$(11,11,2)=TM\$(6,4)
 TM\$(11,11,1)=TM\$(6,5)
 TM\$(11,11,0)=TM\$(6,6)
 TM\$(11,11,15)=D1
 TM\$(11,11,14)=TM\$(13,1)
 TM\$(11,11,13)=0
 TM\$(11,11,12)=0
 TM\$(11,11,11)=TM\$(15,1)
 TM\$(11,11,10)=D1+2.*D2
 TM\$(11,11,9)=TM\$(13,2)
 TM\$(11,11,8)=2.*D1+D2
 TM\$(11,11,7)=TM\$(14,2)
 TM\$(11,11,6)=D1+D2
 TM\$(11,11,5)=TM\$(15,2)
 TM\$(11,11,4)=0
 TM\$(11,11,3)=TM\$(13,3)
 TM\$(11,11,2)=D2
 TM\$(11,11,1)=TM\$(14,3)
 TM\$(11,11,0)=0
 TM\$(11,11,15)=TM\$(15,3)
 TM\$(11,11,14)=D2+D3
 TM\$(11,11,13)=TM\$(13,4)
 TM\$(11,11,12)=D2+2.*D3
 TM\$(11,11,11)=TM\$(14,4)
 TM\$(11,11,10)=2.*D2+D3
 TM\$(11,11,9)=TM\$(15,4)
 TM\$(11,11,8)=0
 TM\$(11,11,7)=TM\$(13,5)
 TM\$(11,11,6)=0
 TM\$(11,11,5)=TM\$(14,5)
 TM\$(11,11,4)=D3
 TM\$(11,11,3)=TM\$(15,5)
 TM\$(11,11,2)=D1+2.*D3
 TM\$(11,11,1)=TM\$(13,6)
 TM\$(11,11,0)=D1+D3
 TM\$(11,11,15)=2.*D1+D3
 TM\$(11,11,14)=TM\$(15,6)

FLU03630
 FLU03640
 FLU03650
 FLU03660
 FLU03670
 FLU03680
 FLU03690
 FLU03700
 FLU03710
 FLU03720
 FLU03730
 FLU03740
 FLU03750
 FLU03760
 FLU03770
 FLU03780
 FLU03790
 FLU03800
 FLU03810
 FLU03820
 FLU03830
 FLU03840
 FLU03850
 FLU03860
 FLU03870
 FLU03880
 FLU03890
 FLU03900
 FLU03910
 FLU03920
 FLU03930
 FLU03940
 FLU03950
 FLU03960
 FLU03970
 FLU03980
 FLU03990
 FLU04000
 FLU04010
 FLU04020
 FLU04030
 FLU04040
 FLU04050
 FLU04060
 FLU04070
 FLU04080
 FLU04090
 FLU04100

FLU04110
 FLU04120
 FLU04130
 FLU04140
 FLU04150
 FLU04160
 FLU04170
 FLU04180
 FLU04190
 FLU04200
 FLU04210
 FLU04220
 FLU04230
 FLU04240
 FLU04250
 FLU04260
 FLU04270
 FLU04280
 FLU04290
 FLU04300
 FLU04310
 FLU04320
 FLU04330
 FLU04340
 FLU04350
 FLU04360
 FLU04370
 FLU04380
 FLU04390
 FLU04400
 FLU04410
 FLU04420
 FLU04430
 FLU04440
 FLU04450
 FLU04460

QZ 00170

TM\$(13,13)=EI
 TM\$(7,13)=TM\$(13,7)
 TM\$(14,17)=0
 TM\$(7,14)=TM\$(14,7)
 TM\$(15,17)=0
 TM\$(7,15)=TM\$(15,7)
 TM\$(13,18)=EI+2.*E2
 TM\$(8,13)=TM\$(13,8)
 TM\$(14,18)=2.*EI+E2
 TM\$(8,14)=TM\$(14,8)
 TM\$(15,18)=EI+E2
 TM\$(8,15)=TM\$(15,8)
 TM\$(13,19)=0
 TM\$(9,13)=TM\$(13,9)
 TM\$(14,19)=EI+E2
 TM\$(9,14)=TM\$(14,9)
 TM\$(15,19)=0
 TM\$(9,15)=TM\$(15,9)
 TM\$(13,10)=EI+2.*E3
 TM\$(10,13)=TM\$(13,10)
 TM\$(14,10)=EI+2.*E3
 TM\$(10,14)=TM\$(14,10)
 TM\$(15,10)=EI+2.*E3
 TM\$(10,15)=0
 TM\$(13,11)=TM\$(13,11)
 TM\$(14,11)=0
 TM\$(11,14)=TM\$(14,11)
 TM\$(15,11)=EI+2.*E3
 TM\$(11,15)=TM\$(15,11)
 TM\$(12,13)=EI+2.*E3
 TM\$(13,12)=EI+2.*E3
 TM\$(14,12)=EI+2.*E3
 TM\$(15,12)=EI+2.*E3
 TM\$(12,15)=EI+2.*E3
 CONST2=1/(4.*DEL)
 TM\$(13,13)=-.5*(B1*B1+C1*C1)*CONST2
 TM\$(13,14)=-.5*(B1*B2+C1*C2)*CONST2
 TM\$(13,15)=-.5*(B1*B3+C1*C3)*CONST2
 TM\$(14,13)=EI+2.*E3
 TM\$(14,14)=EI+2.*E3
 TM\$(14,15)=EI+2.*E3
 TM\$(15,13)=EI+2.*E3
 TM\$(15,14)=EI+2.*E3
 TM\$(15,15)=EI+2.*E3

C

C


```

U(1)=U1
U(2)=U2
U(3)=U3
U(4)=U4
U(5)=U5
U(6)=U6
V(1)=V1
V(2)=V2
V(3)=V3
V(4)=V4
V(5)=V5
V(6)=V6
NT(1)=N1
NT(2)=N3
NT(3)=N5

```

```

QZ 00180
QZ 00190
QZ 00200
QZ 00210
QZ 00220
QZ 00230
QZ 00240
QZ 00250
QZ 00260
QZ 00270
QZ 00280
QZ 00290
QZ 00300

```

```

CONST3=1./DEL*4.*60.
QZ1(1,1)=0.0
QZ1(2,1)=56.*(B2*C1-B1*C2)*CONST3
QZ1(2,2)=0.0
QZ1(3,1)=-8.*(B2*C1-B1*C2)*CONST3
QZ1(3,2)=12.*(B2*C1-B1*C2)*CONST3
QZ1(3,3)=0.0
QZ1(4,1)=12.*(B3*C1+B2*C2-B1*C3-B1*C2)*CONST3
QZ1(4,2)=16.*(B2*C1-B1*C2)+32.*(B3*C2+B3*C1-B2*C3-B1*C3)*CONST3
QZ1(4,3)=12.*(B3*C2-B2*C3)*CONST3
QZ1(4,4)=0.0
QZ1(5,1)=-8.*(B3*C1-B1*C3)*CONST3
QZ1(5,2)=-4.*(B3*C2-B2*C3)*CONST3
QZ1(5,3)=12.*(B3*C2-B2*C3)*CONST3
QZ1(5,4)=0.0
QZ1(6,1)=56.*(B3*C1-B1*C3)*CONST3
QZ1(6,2)=96.*(B3*C2-B2*C3)+32.*(B1*C2+B3*C1-B2*C3-B1*C3)*CONST3
QZ1(6,3)=-4.*(B1*C2-B2*C3)*CONST3
QZ1(6,4)=16.*(B1*C3-B3*C1)+32.*(B3*C2+B1*C2-B2*C3-B2*C1)*CONST3
QZ1(6,5)=12.*(B1*C3-B3*C1)*CONST3
QZ1(6,6)=0.0
QZ2(1,1)=0.0
QZ2(2,1)=12.*(B2*C1-B1*C2)*CONST3
QZ2(2,2)=0.0
QZ2(3,1)=-8.*(B2*C1-B1*C2)*CONST3
QZ2(3,2)=56.*(B2*C1-B1*C2)*CONST3
QZ2(3,3)=0.0
QZ2(4,1)=-8.*(B3*C1-B1*C3)-4.*(B2*C1-B1*C2)*CONST3

```

```

QZ 00340
QZ 00350
QZ 00360

```

```

QAR00030
QAR00040
QAR00050
QAR00060
QAR00070
QAR00080
QAR00090
QAR00100
QAR00110
QAR00120
QAR00130
QAR00140
QAR00150
QAR00160
QAR00170
QAR00180
QAR00190
QAR00200
QAR00210
QAR00220
QAR00230
QAR00030
QAR00040
QAR00050
QAR00060
QAR00070
QAR00080
QAR00090

```



```

QZ2(4,2)=(96.*(B3*C1-B1*C3)+32.*(B2*C1+B3*C2-B1*C2-B2*C3))*CONST3
QZ2(4,3)=56.*(B3*C2-B2*C3)*CONST3
QZ2(4,4)=0.0
QZ2(5,1)=-4.*(B3*C1-B1*C3)*CONST3
QZ2(5,2)=-4.*(B3*C2-B2*C3)-8.*(B3*C1-B1*C3))*CONST3
QZ2(5,3)=-8.*(B3*C2-B2*C3)*CONST3
QZ2(5,4)=-12.*(B3*C2-B2*C3)*CONST3
QZ2(5,5)=0.0
QZ2(6,1)=12.*(B3*C1-B1*C3)*CONST3
QZ2(6,2)=16.*(B1*C2-B2*C1)+32.*(B3*C1+B3*C2-B1*C2-B2*C3))*CONST3
QZ2(6,3)=12.*(B1*C2+B3*C2-B2*C1-B2*C3)*CONST3
QZ2(6,4)=16.*(B1*C2-B2*C3)+32.*(B1*C3+B1*C2-B3*C1-B2*C1))*CONST3
QZ2(6,5)=12.*(B1*C3-B3*C1)*CONST3
QZ2(6,6)=0.0
QZ3(1,1)=0.0
QZ3(2,1)=12.*(B2*C1-B1*C2)*CONST3
QZ3(2,2)=0.0
QZ3(3,1)=-4.*(B2*C1-B1*C2)*CONST3
QZ3(3,2)=12.*(B2*C1-B1*C2)*CONST3
QZ3(3,3)=0.0
QZ3(4,1)=-4.*(B3*C1-B1*C3)-8.*(B2*C1-B1*C2))*CONST3
QZ3(4,2)=16.*(B3*C2-B2*C3)+32.*(B2*C1+B3*C1-B1*C2-B1*C3))*CONST3
QZ3(4,3)=12.*(B3*C2-B2*C3)*CONST3
QZ3(4,4)=0.0
QZ3(5,1)=-8.*(B3*C1-B1*C3)*CONST3
QZ3(5,2)=12.*(B3*C2-B2*C3+B3*C1-B1*C3))*CONST3
QZ3(5,3)=-8.*(B3*C2-B2*C3)*CONST3
QZ3(5,4)=56.*(B3*C2-B2*C3)*CONST3
QZ3(5,5)=0.0
QZ3(6,1)=12.*(B3*C1-B1*C3)*CONST3
QZ3(6,2)=16.*(B3*C1-B1*C3)+32.*(B1*C2+B3*C2-B2*C1-B2*C3))*CONST3
QZ3(6,3)=-8.*(B1*C2-B2*C1)-4.*(B3*C2-B2*C3)*CONST3
QZ3(6,4)=-96.*(B1*C2-B2*C1)+32.*(B3*C2+B1*C3-B2*C3-B3*C1))*CONST3
QZ3(6,5)=56.*(B1*C3-B3*C1)*CONST3
QZ3(6,6)=0.0

```

C C

```

DO 57 JA=1,14
DO 57 JB=1,3
ICHECK=NT(JB)-NI(JA)
IF(ICHECK.EQ.0) GO TO 58
GO TO 57
IF(JB-2) 60,70,80
QPRM=0.0
DO 61 KO=1,6
DO 61 KM=1,KO
QPRM=QPRM+(U(KO)*V(KM)-U(KM)*V(KO))*QZ1(KO,KM)
CONTINUE

```

58 60 61


```

70 Q(NCP(NT(JB)))=QPRM+Q(NCP(NT(JB)))
   GO TO 57
   QPRM=0.0
   DO 71 KN=1,6
   DO 71 KL=1,KN
   QPRM=QPRM+(U(KN)*V(KL)-U(KL)*V(KN))*QZ2(KN,KL)
   CONTINUE
71 Q(NCP(NT(JB)))=QPRM+Q(NCP(NT(JB)))
   GO TO 57
80 CERM=0.0
   DO 81 KP=1,6
   DO 81 KQ=1,6
   QPRM=QPRM+(U(KP)*V(KQ)-U(KQ)*V(KP))*QZ3(KP,KQ)
   CONTINUE
81 Q(NCP(NT(JB)))=QPRM+Q(NCP(NT(JB)))
57 CONTINUE
   QZC(1)=C1*C1
   QZC(2)=2.*C1*C2
   QZC(3)=C2*C2
   QZC(4)=2.*C2*C3
   QZC(5)=C3*C3
   QZC(6)=2.*C1*C3
   QZB(1)=B1*B1
   QZB(2)=2.*B1*B2
   QZB(3)=B2*B2
   QZB(4)=2.*B2*B3
   QZB(5)=B3*B3
   QZB(6)=2.*C1*C3
   NLCY(1)=17
   NLCY(2)=18
   NLCY(3)=20
   NLCY(4)=22
   NRCY(1)=30
   NRCY(2)=33
   NRCY(3)=34
   NRCY(4)=36
   CONST4=A/(4.*DEL**2)
   DO 513 LA=1,4
   JCHECK=K-NLCY(LA)
   KCHECK=K-NRCY(LA)
   IF(JCHECK.EQ.0) GO TO 517
   IF(KCHECK.EQ.0) GO TO 519
   GO TO 513
517 THETA=ATAN((YC(NT(3))-YC(NT(2)))/(XC(NT(3))-XC(NT(2))))
   THETA1=THETA-2.*ATAN(1.)
   SLIJ=SQRT((YC(NT(3))-YC(NT(2)))**2+(XC(NT(3))-XC(NT(2)))**2)
   XHAT=COS(THETA1)
   YHAT=SIN(THETA1)

```

QZ 00550
QZ 00560
QZ 00570
QZ 00580
QZ 00590

QZ 00630
QZ 00640
QZ 00650

GO 00020
GO 00030
GO 00040
GO 00050
GO 00060
GO 00070
GO 00080
GO 00090
GO 00100
GO 00110
GO 00120
GO 00130
GO 00140
GO 00150
GO 00160
GO 00170
GO 00180


```

PART1=0.0
PART2=0.0
TPART=0.0
DO 523 LB=1,6
PART1=PART1+(U(LB)*QZB(LB))*CONST4
PART2=PART2+(V(LB)*QZC(LB))*CONST4
CONTINUE
TPART=PART1+PART2
Q(NCP(NT(2)))=Q(NCP(NT(2)))+TPART*SLIJ
Q(NCP(NT(3)))=Q(NCP(NT(3)))+TPART*SLIJ
GC TO 513
523
THETA2=ATAN((YC(NT(1)))-YC(NT(2)))/(XC(NT(2))-XC(NT(1))))
THETA1=6.*ATAN(1.)-THETA2
SLIJ=SQRT((YC(NT(1)))-YC(NT(2)))**2+(XC(NT(1)))-XC(NT(2)))**2)
XHAT=COS(THETA1)
YHAT=SIN(THETA1)
TPART=0.0
PART1=0.0
PART2=0.0
DO 521 LB=1,6
PART1=PART1+(U(LB)*QZB(LB))*CONST4
PART2=PART2+(V(LB)*QZC(LB))*CONST4
CONTINUE
TPART=PART1+PART2
Q(NCP(NT(1)))=Q(NCP(NT(1)))+TPART*SLIJ
Q(NCP(NT(2)))=Q(NCP(NT(2)))+TPART*SLIJ
CONTINUE
CONTINUE
N(1)=N1
N(2)=N2
N(3)=N3
N(4)=N4
N(5)=N5
N(6)=N6
N(7)=N7
N(8)=N8
N(9)=N9
N(10)=N10
N(11)=N11
N(12)=N12
N(13)=N13
N(14)=N14
N(15)=N15
DO 200 I$=1,15
I= N(I$)
DO 200 J$=1,15
J= N(J$)
TM(I,J)=TM(I,J)+TM$(I$,J$) .

```

523

519

521

513
185

GO 00210
GO 00220
GO 00240
GO 00250
GO 00260
GO 00270
GO 00280
GO 00290
GO 00300
GO 00320
FLU04470
FLU04480
FLU04490
FLU04500
FLU04510
FLU04520
FLU04530
FLU04540
FLU04550
FLU04560
FLU04570
FLU04580
FLU04590
FLU04600
FLU04610
FLU04620
FLU04630
FLU04640
FLU04650
FLU04660
FLU04670


```

200 CONTINUE
300 CONTINUE
   IF(NNQXY.EQ.0) GO TO 310
   DO 310 I=1,NNQXY
     RHS(NQS(I))=RHS(NQS(I))+Q(NQS(I))
     RHS(NQS(I)+NN)=RHS(NQS(I)+NN)+Q(NQS(I)+NN)
   IF(I-NNPQ)309,309,310
309 RHS(NCP(NPS(I+NNPS)))=RHS(NCP(NPS(I+NNPS)))+Q(NCP(NPS(I+NNPS)))
310 CONTINUE
320 CONTINUE
   CALL SOLMIX(MM,IM,T,RHS,NTOTVP,NVIS,NTOTQ,NQIS,B,Z,C)
   WRITE(NWRITE,2000)
   NTEST=0
   DO 322 J=1,MM
     ESPILA=ABS(T1(J)-T(J))
     IF(ESPILA-.001)322,324,324
322 CONTINUE
324 NTEST=100
   DO 325 I=1,NN
     IV=I+NN
     IQ=I+2*NN
     T1(I)=
       T(I)
     Q(I)=RHS(I)
     T1(IV)=
       T(IV)
     Q(IV)=RHS(IV)
     IF(MM-IQ)2223,2222,2222
     T1(IQ)=
       T(IQ)
     Q(IQ)=RHS(IQ)
   WRITE(NWRITE,2300)I,T(I),IV,T(IV),IQ,T(IQ),Q(I),Q(IV),Q(IQ)
   GC TO 325
2223 WRITE(NWRITE,2301)I,T(I),IV,T(IV),Q(I),Q(IV)
325 CONTINUE
   IF(NTEST.NE.100) GO TO 177
500 FORMAT(110)
1005 FORMAT(6X,A4,I10,2F10.0)
1006 FORMAT(6X,A4,I10,2F10.0)
1010 FORMAT(7110)
1015 FORMAT(6X,A4,I10,F10.0)
1016 FORMAT(6X,A4,I10,F10.0)
1020 FORMAT(110,2F10.0)
1025 FORMAT(6X,A4,I10,F10.0)
1030 FCFORMAT(6X,A4,2I10,2F10.0)
1035 FORMAT(5X,'NO. OF CORNER NODES=',I3,/,
15X,'NO. OF SUMMARY OF NODAL COORDINATES',/,
17X,'I',I,12X,X(I),I,12X,Y(I),/,
1045 FORMAT(5X,I3,2(7X,F10.3))

```

FLU04680
 FLU04690
 FLU04700
 FLU04710
 FLU04720
 FLU04730

FLU04740
 FLU04750
 FLU04760
 FLU04770

FLU04780
 FLU04790
 FLU04800
 FLU04810

FLU04820

FLU04860

FLU04880
 FLU04890
 FLU04900
 FLU04910
 FLU04920
 FLU04930
 FLU04940
 FLU04950
 FLU04960
 FLU04970
 FLU04980
 FLU04990
 FLU05000
 FLU05010


```

1050 FORMAT(5X,'LISTING OF SYSTEM TOPOLOGY',//,5X
1,ELEMENT NUMBER',20X,'NODE NUMBERS',//)
1055 FORMAT(5X,I3,10X,6(5X,I3))
1060 FORMAT(7X,'NODES WHERE VELOCITIES ARE SPECIFIED',
//,8X,I1,5X,'NODE',5X,'U VELOCITY',5X,'V VELOCITY',//)
1065 FORMAT(2X,2(4X,I3),3X,F12.3,F12.3)
1070 FORMAT(5X,'SPECIFIED RIGHT HAND SIDE I.E. QX AND QY',
//,2X,'NODE',5X,'QX',5X,'QY',//)
1071 FORMAT(5X,'SPECIFIED RIGHT HAND SIDE FOR PRESSURE NODES, I.E. QZ',
//,2X,'NODE',5X,'QZ',//)
1072 FORMAT(2X,2(4X,I3),3X,F12.3)
1075 FORMAT(5X,I3,2(10X,F12.3))
1080 FORMAT(5X,'NODES WHERE PRESSURE IS SPECIFIED',
//,5X,I1,5X,'NODE',10X,'PRESSURE',//)
1085 FORMAT(5X,I3,3X,I3,10X,F12.3)
2300 FORMAT(6X,3(I3,5X,E13.5,5X),3(E13.5,3X))
2301 FORMAT(6X,2(I3,5X,E13.5,5X),26X,2(E13.5,3X))
2000 FORMAT(3X,'NODE NO.',3X,'T(I)',5X,'X-COORD',5X,'NODE NO.',2X,'T(J)',2
1X,'Y-COORD',5X,'NODE NO.',4X,'T(I)',9X,'Q(I)' X',17X,'Q(I)' Y',12
2 X',Q(I)' P')
2020 FORMAT(1H1,5X,'THIS IS A NON-LINEAR PROBLEM',//)
STOP
END

```

FLU0505020
 FLU0505030
 FLU0505040
 FLU0505050
 FLU0505060
 FLU0505070
 FLU0505080
 FLU0505090
 PRE00200
 PRE00210
 PRE00220
 FLU05100
 FLU05110
 FLU05120
 FLU05130

FLU05210
 FLU05220
 FLU05230


```

SUBROUTINE SOLMIX(N,A,X,Y,NX,LISTX,NY,LISTY,B,Z,C)
DIMENSION A(N,N),X(N),Y(N),Z(NY),C(NY)
IF(N.EQ.(NX+NY)) GO TO 100
WRITE(6,111) N,NX,NY
FORMAT(10X,'N=',I2,10X,'NX=',I2,10X,'NY=',I2)
111 STOP
100 CONTINUE
IF(NX.NE.0) GO TO 120
CALL SOLVE(N,A,Y,X)
RETURN
120 CONTINUE
IF(NY.NE.0) GO TO 140
DO 130 I=1,N
Y(I)=0.
DO 130 J=1,N
Y(I)=Y(I)+A(I,J)*X(J)
130 Y(I)=Y(I)+A(I,J)*X(J)
140 CONTINUE
DO 200 I=1,NY
DO 200 J=1,NY
B(I,J)=A(LISTY(I),LISTY(J))
DO 300 I=1,NY
C(I)=Y(LISTY(I))
DO 300 J=1,NX
C(I)=C(I)-A(LISTY(I),LISTX(J))*X(LISTX(J))
CALL SOLVE(NY,B,C,Z)
DO 400 I=1,NY
X(LISTY(I))=Z(I)
DO 800 I=1,NX
C(I)=0.
DO 600 J=1,NY
C(I)=C(I)+A(LISTX(I),LISTY(J))*X(LISTY(J))
DO 700 J=1,NX
C(I)=C(I)+A(LISTX(I),LISTX(J))*X(LISTX(J))
800 Y(LISTX(I))=C(I)
RETURN
END

```

SOL000010
 SOL000020
 SOL000030
 SOL000040
 SOL000050
 SOL000060
 SOL000070
 SOL000080
 SOL000090
 SOL000100
 SOL000110
 SOL000120
 SOL000130
 SOL000140
 SOL000150
 SOL000160
 SOL000170
 SOL000180
 SOL000190
 SOL000200
 SOL000210
 SOL000220
 SOL000230
 SOL000240
 SOL000250
 SOL000260
 SOL000270
 SOL000280
 SOL000290
 SOL000300
 SOL000310
 SOL000320
 SOL000330
 SOL000340
 SOL000350
 SOL000360
 SOL000370
 SOL000380
 SOL000390


```

SUBROUTINE SOLVE(N,A,C,X)
  DATA NWRITE/6/
  DIMENSION A(N,N),X(N),C(N)
  DO 400 K=1,N
    BIG = ABS(A(K,K))
    IBIG = K
    DO 100 I=K,N
      SIZE = ABS(A(I,K))
      IF(SIZE.LT.BIG) GO TO 100
    BIG=SIZE
    IBIG=I
  100 CONTINUE
    IF(K.EQ. IBIG) GO TO 280
    DO 200 J=K,N
      ABIG = A(IBIG,J)
      A(IBIG,J)=A(K,J)
    200 A(K,J)= ABIG
      CBIG = C(IBIG)
      C(K)=CBIG
    280 CONTINUE
    IF(A(K,K).EQ.0.) GO TO 600
    DO 350 I=1,N
      IF(I.EQ.K) GO TO 350
      RATIO = A(I,K)/A(K,K)
      DO 300 J=K,N
        A(I,J)=A(I,J)-RATIO*A(K,J)
        CALL OVERFL(IQ)
        IF(IQ.EQ.2)GO TO 301
      WRITE(6,98)
    98 FORMAT(1X,IQ,I,J,K,A(I,J),A(K,J),RATIO,A(K,J)
    99 FORMAT(1X,IQ,I,J,K,A(I,J),A(K,J),RATIO
    99 IF IQ=1 OVERFLOW.....IQ=3 UNDERFLOW
    301 CONTINUE
    300 C(I) = C(I) -RATIO*C(K)
    350 CONTINUE
    400 CONTINUE
    DO 500 K=1,N
      X(K) = C(K)/A(K,K)
    500 RETURN
    600 WRITE(6,666)
    666 FORMAT(10X,'SINGULAR MATRIX')
    700 X(I) = 0.
    2 WRITE(NWRITE,2)K
      FORMAT(6X,'K=',I5)

```

SOL00010
 SOL00020
 SOL00030
 SOL00040
 SOL00050
 SOL00060
 SOL00070
 SOL00080
 SOL00090
 SOL00100
 SOL00110
 SOL00120
 SOL00130
 SOL00140
 SOL00150
 SOL00160
 SOL00170
 SOL00180
 SOL00190
 SOL00200
 SOL00210
 SOL00220
 SOL00230
 SOL00240
 SOL00250
 SOL00260

RATIO')

SOL00270
 SOL00280
 SOL00290
 SOL00300
 SOL00310
 SOL00320
 SOL00330
 SOL00340
 SOL00350
 SOL00360

RETURN
END

SOL00380

BIBLIOGRAPHY

1. Kenneth H. Huebner, The Finite Element Method for Engineers, Wiley, 1975.
2. Office of Naval Research, PROJECT SQUID, by W.H.Stevenson and H.D.Thompson, 9-10 March 1972.
3. C. Taylor and P. Hood, "A Numerical Solution of the Navier-Stokes Equations Using the Finite Element Technique", Computers Fluids, Vol. I, No. 1, 1973.
4. 30th Annual National Forum of the American Helicopter Society, Laser Velocimeter Measurements of the Helicopter Rotor Induced Flow Field, by J.C. Biggers and K.L. Orlaff, May 7-9, 1974.

INITIAL DISTRIBUTION LIST

	No. Copies
1. Defense Documentation Center Cameron Station Alexandria, Virginia 22314	2
2. Library, Code 0212 Naval Postgraduate School Monterey, California 93940	2
3. Department Chairman, Code 57 Department of Aeronautics Naval Postgraduate School Monterey, California 93940	1
4. Professor D. J. Collins, Code 57Co Department of Aeronautics Naval Postgraduate School Monterey, California 93940	1
5. LT Terry Scott Wanner, USN 6414 W. Wicklow Circle Colorado Springs, Colorado 80907	1
6. Dr. H. J. Mueller Code 310 Naval Air Systems Command Washington, D. C. 20361	1

16 JAN 75
30 JAN 80

26166

Thesis

W227 Wanner
c.1

166445

Laser doppler anemom-
eter measurement and
analytical comparison of
flow around a cylinder at
low Reynolds number.

T
W

16 JAN 75
30 JAN 80

26166

Thesis

W227 Wanner

c.1

Laser doppler anemom-
eter measurement and
analytical comparison of
flow around a cylinder at
low Reynolds number.

166445

thesW227

Laser doppler anemometer measurement and



3 2768 001 92949 0

DUDLEY KNOX LIBRARY